EUROPEAN ORGANIZATION FOR NUCLEAR RESEARCH

CERN-LEP-VA/87-63

THE EFFECT OF CLEANING AND OTHER TREATMENTS ON THE VACUUM PROPERTIES OF TECHNOLOGICAL MATERIALS USED IN ULTRA-HIGH VACUUM

by

A.G. Mathewson

ABSTRACT

Methods of producing atomically clean surfaces applicable to technological materials and large vacuum vessels where the surface area may attain tens or hundreds of square metres are described.

As well as chemical cleaning methods, the efficiency of treatments such as in situ glow discharge cleaning or heating to high temperature in vacuo are investigated.

The techniques used to evaluate and compare the various treatments included thermal outgassing, Auger electron spectroscopy for chemical analysis of the surface and near surface, ion, electron and x-ray induced neutral gas desorption, measurement of the quantity of desorbable surface gas by argon glow discharge and scanning electron microscope examination of the surface.

In addition, by flash desorption, the binding energies of CO on some stainless steels were measured along with the roughness factor of the surface which gives a measure of the real surface area on which gas may be adsorbed.

Geneva, November 1987

Invited paper presented at the Xth Italian National Congress on Vacuum Science and Technology, Stresa, Italy, 12-17 October 1987.

1. INTRODUCTION

In vacuum systems such as electron and proton storage rings, the base pressure after bakeout at temperatures up to 300°C for 24 hours can reach the 10^{-12} Torr range[1]. Low ultimate pressures in no way imply that the surface is clean, i.e. devoid of gas. It only means that the binding energies of the remaining adsorbed surface gases after bakeout are high enough to give a low thermal outgassing rate Q at room temperature and that the pumping speed of the pumps S is high enough (and, of course, their vacuum limit low enough) to maintain this low pressure. The pressure P inside the system is given by the simple expression

$$P = Q/S.$$

However, when these machines are in operation the inside walls of the vacuum chamber are subjected to energetic ion, photon or electron bombardment (eV to keV) which desorbs the tightly bound surface gas which may result in large increases in pressure detrimental to the running of the machine[2].

In this invited paper on the effect of cleaning and other treatments on the vacuum properties of technological materials used in ultra-high vacuum, I shall describe the methods which we, at CERN, have used for investigating surfaces and the techniques we have developed for removing absorbed gas. I shall be talking about cleaning procedures and treatments applicable to large vacuum systems fabricated from multi-component alloys such as 316 L + N stainless steel, or Al 6060 whose surface areas may extend to hundreds of square metres and about the methods used to control the quality of the various treatments.

2. RESIDUAL GAS COMPOSITION

In a clean, baked, all-metal ultra-high vacuum system with a pressure in, for example, the 10^{-11} Torr range, the residual gas is usually composed mainly of H_2 (~ 82%) with traces of CH_4 (4%), CO (9.5%) and CO_2 (4.5%). A typical spectrum is shown in Figure 1a.

The composition of the residual gas is, of course, a reflection of the nature of the gas species adsorbed on the surface but gives little indication of the quantity since, as stated previously, molecules in high binding energy states desorb little at room temperature.

Under energetic particle bombardment the gases desorbed are H_2, CH_4, CO and CO_2. Although visible in the residual gas H_2O is not desorbed.

The pressure in the vacuum system may rise by a factor of 10^3 and have a composition drastically different from the initial.

A typical spectrum from a vacuum system subjected to synchrotron radiation where the pressure has risen from 7×10^{-11} Torr to 5×10^{-7} Torr is shown in Figure 1b. There it is seen that the composition is now 31% H_2, 7% CH_4, 24% CO and 38% CO_2, i.e. apart from H_2 the principal contaminating gases in the vacuum system are all C based.

3. DEFINITION OF CLEANLINESS

The definition of a clean surface for vacuum is subjective in that it depends very much on the environment to which the surface is exposed and the use to which it is put. We may adopt the definition of Allen[3] which states that an atomically clean surface is one which is free of all but a few per cent of a single monolayer of foreign atoms either absorbed on or substitionally replacing surface atoms of the parent lattice. Alternatively, we may define a clean surface to be one which desorbs less than a certain number and/or species of gas molecules due to thermal effects or to incident electrons, ions or photons.

Depending on the circumstances and the degree of cleanliness required, the maximum tolerable number of gas molecules desorbed must be specified as must the energy of the bombarding particles and the ion species.

It would, of course, be advantageous to find a treatment or treatments which would reduce both the thermal outgassing rate and the quantity of desorbable surface gas.

4. TESTING OF CLEANING METHODS

To test the cleaning methods we shall describe, the thermal outgassing rates of small samples and also complete vacuum chambers were measured. In addition, they were subjected to electron, ion or photon bombardment and the number and identity of the desorbed gas molecules determined. An apparatus in which this can be done is shown schematically in Figure 2, a fuller description may be found in references 4) and 5). In this equipment, samples can be subjected to electron, K^+ and $^{15}N_2$ ion bombardment with energies up to 3 keV. Complete vacuum chambers were subjected to photon bombardment in a dedicated beam line of the synchrotron radiation source at L.U.R.E., Orsay, France[6].

The composition of the surface may be conveniently imaged and analysed using Scanning Auger Electron Spectroscopy[7] (A.E.S.). By means of this analysis technique the elements present in the first 3 or 4 monolayers of the surface may be identified. As well as identification a quantitative measurement is provided and in conjunction with inert gas ion bombardment, which removes the sample surface layer by layer, a plot of elemental concentration versus depth can be obtained.

5. A CHEMICAL SOLVENT PRECLEANING PROCEDURE

In all cases before final cleaning all materials must be subjected to a precleaning to remove gross contamination such as oil and grease and particulate matter of all types. Such a procedure never provides an atomically clean surface[8] since traces of the cleaning solutions wll always remain and, of course, exposure to air results in adsorption of water vapour, CO_2, etc.

A reasonably effective precleaning procedure used at CERN consists of the following steps:

(a) Removal of gross contamination and machining oils
(b) Perchloroethylene (C_2Cl_4) vapour degreasing (121°C)
(c) Ultrasonic cleaning in alkaline detergent (pH = 11)
(d) Rinsing in cold, demineralized water
(e) Drying in a hot air oven at 150°C.

There are, of course, a multitude of similar procedures using other chlorinated and fluorinated hydrocarbons such as trichloroethylene and freon, and alcohols. The above process we have found to be effective in precleaning pure Ti, Ti alloy (73 Ti 13 V 11 Cr 3 Al), Inconel 600, Inconel 625, Cu and 316 L + N stainless steel which have been contaminated with the usual cutting oils and greases. However, it must be emphasized that there is no universal solvent for all possible contaminants. Before defining a precleaning procedure the contaminants to be removed must first be identified.

The efficiency of the above precleaning procedure may be checked by A.E.S. In Figure 3 (top) is shown the Auger spectrum from a previously uncleaned 316 L + N stainless steel specimen. The surface is heavily contaminated with C (~ 82 at.%). From the peak shape the C appears to be in the form of graphite[9] but oil and other complicated hydrocarbons are certainly also present on the uncleaned surface. Traces of S, Cl, Ca and Na are observed. The underlying Fe, Cr and Ni, the main constituants of 316 L + N stainless steel, are obscured by this contaminating layer. The O is not necessarily an impurity but is an essential component of the stainless steel passivation layer, however it must be remembered that O from adsorbed H_2O, CO and CO_2 will also contribute to the observed O peak.

The second spectrum from the top in Figure 3 shows the result of only degreasing a similar uncleaned 316 L + N stainless steel sample in perchloroethylene vapour. The C contamination is greatly reduced (~ 44 at.%) revealing the underlying Fe, Cr and Ni. However, traces of S, Ca and Na still remain, K is not removed and Clf rom the vapour degreasing process is evident.

Passing an uncleaned 316 L + N sample through all four stages of the precleaning procedure results in the Auger spectrum second from the bottom in Figure 3. The C contamination is further reduced (~ 28 at.%) but still vastly in excess of the bulk C content (0.016% by weight). Some Ca is still present on the surface but the S, Cl and Na are now barely detectable. The Cu - not a constituent of 316 L + N stainless steel and hence a true contaminant - which appeared on the surface, was traced to the

detergent bath. It was due to manual rubbing of the surface of some Cu parts with an abrasive cloth while still in the detergent bath resulting in some Cu remaining in suspension in the detergent.

The bottom spectrum of Figure 3 illustrates the necessity of using demineralized water in the rinsing stage of the cleaning process. If ordinary tap water is used, as in this case, appreciable quantities of Ca (~ 36 at.%), the origin of which is most likely $CaCO_3$, are observed on the surface.

6. FLASH DESORPTION

The binding energies of surface species may be measured by the technique of flash desorption in which a sample of say, stainless steel, is heated in vacuo at a known rate and the partial pressures of the gases released during the flash recorded. The temperatures at which pressure peaks in this desorption spectrum occur are related to the binding energy of the desorbed species. The measurement of these binding energies is of interest since it can be seen whether increasing bakeout temperatures from 300°C to perhaps 350°C or 400°C can significantly deplete the populations of the more tightly bound surface states.

The theory of flash desorption is well covered in the literature[10] so only the final expression from which the binding energies may be calculated will be given. The relationship between the binding energy E and the temperature T_p at which the maximum desorption occurs is given by

$$\frac{E}{kT_p^2} = \frac{\nu}{\beta} \exp\left(\frac{-E}{kT_p}\right)$$

where k is Boltzmann's constant

ν is the rate constant (~ 10^{13} s^{-1})

and β is the rate of change of sample temperature.

Another useful expression is the time τ required to reduce the initial surface concentration of a state of binding energy E by 1/e by heating at a temperature T°K and is

$$\tau = \nu^{-1} \exp\left(\frac{-E}{kT}\right)$$

with ν normally = 10^{13} s^{-1}.

In Table I are shown values of τ for various binding energies between 0.9 eV and 2.8 eV and for temperatures of 200°C, 300°C and 400°C. For a value of the rate constant $\nu = 10^{12}$ s^{-1}, the times would, of course, be a factor of 10 higher. Such a value for ν cannot be excluded.

The experimental equipment is shown schematically in Fig. 4 and a complete description will be found in reference 11).

Three types of stainless steel, all cleaned by the chemical solvent method described above, were investigated and in all three thermal diffusion of N_2 from the bulk tended to mask the thermal desorption spectra above about 600°C. The diffusion activation energy of this bulk N_2 was measured and found to be 1.87 eV (43 kcal $mol.^{-1}$) a value which corresponds closely to the quoted N_2 migration activation energy in austenitic Fe of 1.75 eV[12] (40.3 kcal $mol.^{-1}$).

In Fig. 5 is shown the flash desorption spectrum of CO from non-degassed 316 L + N stainless steel. Three desorption peaks are visible in the first flash, i.e. α, ß and γ at 110, 395 and 517°C with corresponding binding energies of 0.97, 1.72 and 2.05 eV. The bulk N_2 diffusion is evident at the higher temperatures. Subsequent flashes revealed that α, ß and states had been depleted but the bulk N_2 diffusion remained.

This clean sample was exposed to 10^{-6} Torr of CO for increasing lengths of time and the spectra shown in Fig. 5 recorded. Only the α and γ states repopulated with CO even after 9.9×10^3 L (1L = 10^{-6} Torr s) of exposure to CO.

Not all samples of the same stainless steel gave identical spectra, the peak positions varying somewhat from sample to sample. However, in Table II is a list of the positively identified CO binding state energies

for the four stainless steel samples studied. The 2.8 eV state on 316 L is marked with a question mark since the exact peak position was difficult to determine due to the large N_2 background.

Baking at 300°C for 24 hours is insufficient to deplete all the CO binding states observed. In Table I it can be seen that at 300°C states with binding energies greater than about 1.7 eV are not depleted. This figure may be even less if the rate constant is lower than 10^{13} s^{-1}. Even at 400°C the 2.0 eV state may remain populated if the rate constant is 10^{12} s^{-1}. Thus even after 400°C bakeouts there will still be CO on the surface which may subsequently desorb under energetic particle bombardment.

7. CLEANING BY HEATING

Atomically clean surfaces of high melting point metals may be easily obtained by heating the material to a high temperature in vacuum. This method is only applicable to those materials whose surface contaminants possess higher vapour pressures than the base material or decompose at temperatures below the melting point of the base metal. However, at elevated temperatures there exists the possibility that the surfaceimpurities may not leave as gaseous species but instead diffuse into the bulk. Alternatively impurities in the bulk may diffuse to the surface. In addition, the mechanical properties of the material may be seriously degraded by the high temperature treatment.

The effect on the surface composition of heating 316 L + N stainless stell to high temperature is shown by the series of Auger spectra in Fig. 6[13]. The surface composition was analyzed at room temperature (25°C) and after heating at 100°C intervals from 100°C to 900°C. The spectra were recorded with the sample at room temperature after heating for one hour. The sample had been precleaned by the method described above before mounting in the Auger system.

The composition of the 316 L + N stainless steel surface after the chemical precleaning is shown by the top spectrum of Figure 6 with the actual percentages for C, O and S shown in Figure 7. The major

contaminants were C (~ 61 at.%) with traces of P (~ 1.5 at.%) from the cleaning, S (~ 1.0 at.%) and Cl (~ 1.0 at.%). Again the O is not considered to be a true contaminant but is a normal component of the metal surface which had, of course, been exposed to air and hence oxidized. Heating the sample from 25°C to 300°C produced almost no change in the surface composition except that chromium was more in evidence. After heating to 400°C and 500°C a decrease in both the O and Fe content of the surface and an increase in the chromium concentration was observed. The C concentration remained relatively static. From 600°C up to 900°C the C and O peaks decreased becoming undetectable at 900°C. However, at 600°C, P and S appeared on the surface having diffused from the interior. At 900°C a C and O free surface is obtained but with bulk S segregated at the surface. The S peak height after heating to 900°C corresponds to about 11 at.%. At 800°C and 900°C the constituents of the stainless steel i.e. Ni, Fe and Cr are clearly seen.

To investigate the temperature dependence of the electron and ion induced neutral gas desorption coefficients, a sample was cleaned and installed in the measuring equipment[13]. After sufficient pumping time to reach a pressure ~ 1 x 10^{-8} Torr, usually about 2 days, a measurement of was made. The complete system was then baked at 150°C for 24 hours to give a good base pressure ~ 2 x 10^{-10} Torr and the desorption coefficients measured again. Sample temperatures higher than these bakeout temperatures were obtained by heating only the sample for 24 hours in this now baked system, then, after cooling, again measuring the desorption coefficients. After the system with the stainless steel sample installed was baked at 150°C, the sample was then heated to 300°C in 50°C steps and from 300°C to 600°C in 100°C steps.

Only H_2, CH_4, CO and CO_2 were seen to be desorbed by electrons or ions from the stainless steel, i.e. apart from the H_2 the desorbed species are C based.

In Figure 8 are shown the temperature dependence of the electron and ion induced desorption coefficients for 316 L + N stainless steel. The K^+ ion induced desorption coefficients at 1400 eV for H_2 and CO (i.e. η_{H_2}

and η_{CO} are largest and of the same order of magnitude. They are followed by ηCO_2 and ηCH_4, both these being about an order of magnitude lower.

For the electron induced desorption the order is somewhat different. The largest is η_{H_2} followed by η_{CO_2} and η_{CO} and finally η_{CH_4}. As can be seen from the figures this order is not strictly maintained over the temperature range of interest but is in general true. The different temperature dependence and different desorption efficiencies for the electrons and ions are explicable in terms of the different desorption mechanisms. Under ion bombardment the desorption takes place by momentum transfer between the incident ion and the adsorbed gas molecule (possibly via the substrate) whereas in electron induced desorption the adsorbed atom is first excited to an antibonding state by the incident electron which interacts with the binding electrons[14].

The general rule is that the higher the bakeout temperature the cleaner is the surface.

8. GLOW DISCHARGE CLEANING

Under the action of ion bombardment, adsorbed surface gas and also metal atoms may be removed by sputtering. Argon is the gas most commonly used because of its inertness and thus inability to react chemically with the surface bombarded. In addition, the higher mass of Ar relative to He and Ne makes the sputtering more efficient[15]. The use of the heavier inert gases Kr and Xe is excluded only on account of their cost.

Ion bombardment of a surface disrupts it greatly and introduces a large number of defects. This, however, is of minor consequence in the cleaning of large vacuum vessels where defects in the surface layers are not necessarily detrimental to their operation. However, some ions will always be implanted in the surface and, after the discharge cleaning has terminated, will tend to diffuse to the surface and desorb thermally providing a source of gas which has to be coped with by the system pumps. This effect can be minimized by degassing the discharge cleaned vessel under vacuum at as high a temperature as possible for some hours after the end of the discharge.

For investigation of the discharge cleaning process a miniature 316 L + N stainless steel discharge cell was placed in the A.E.S. system. As shown in Figure 9 a 316 L + N stainless steel specimen could be rotated from its position integral with the discharge cell wall to a position suitable for analysis via A.E.S. without breaking the vacuum. Thus the cleaning effect of the argon ion bombardment could be monitored in situ after various ion doses. The discharge cell was not deliberately heated but the energy transferred from the discharge to the cell raised its temperature to about 100°C.

The Auger spectrum in Fig. 10 (top) shows the state of the specimen, i.e. the chamber wall before discharge. Both cell and specimen had been subjected to the precleaning process described above. The main contaminant is C with some Ca, Cl, P and Cu.

The bottom spectrum is taken from the discharged specimen after an argon ion dose of 1.6×10^{19} ions cm^{-2}. Further doses did not change the spectrum. One can now clearly see the base constituents of the steel such as Fe, Cr, Ni, Mo and even N_2. However, some C is still present but in the form of carbide shown by the characteristic peak shape[9]. The O peak has greatly diminished and the low energy Fe and Ni peaks are very strong indicating that very little overlying contamination is present.

In addition to surface gas the stainless steel itself is sputtered and all insulators and windows in such a discharge become coated with a layer of metal. However, because of the geometry, i.e. radial ion bombardment, the sputtered material is not removed from the chamber but is merely transported from side to side with only the volatile components being removed. Carbon itself is not volatile and is therefore not completely removed for this reason.

The effect of introducing 10% oxygen into the argon gas used in the discharge is spectacular[16]. Apart from some implanted argon and, of course, some oxygen, an atomically clean surface free of C is obtained after a dose of only 1×10^{18} ions cm^{-2} compared to 1.6×10^{19} ions cm^{-2} with pure argon which even then did not remove all the C. The before and

after argon/10% oxygen discharge Auger spectra are shown in Fig. 11. The effect of the oxygen is obviously to oxidise the surface C forming CO and CO_2 which is then pumped from the system.

During the pure argon discharge cleaning of the stainless vacuum chambers of the CERN proton storage rings, it was observed that even after baking a vacuum chamber at 400°C for 27 hours the initiation of the discharge in the vacuum chamber always resulted in a distinct rise in pressure ($\Delta P = 5 \times 10^{-2}$ Torr at a base pressure of 1×10^{-2} Torr of argon). Thus the argon ions are desorbing gases which have low desorption rates at 400°C namely large binding energies. Analysis of these discharge-induced pressure rises would give some useful information concerning what was being desorbed from the vacuum chamber surface and in addition could be used for testing the stability of different surfaces under ion bombardment and the efficiency of different cleaning methods including the discharge itself.

The equipment for analysis of the gas discharge induced pressure rises is shown in Figure 12. A more complete description is given in reference 17).

It was found that discharge cleaning with the chamber at 300°C was more efficient than at room temperature. The composition and time dependence of a typical pressure rise are shown in Figure 13 for a 316 L + N stainless steel test chamber at 300°C. The only gaseous species desorbed are CO, H_2, CH_4 and CO_2. The relative surface concentrations of these gases were obtained from Figure 12 by integrating each curve with respect to time but for CO stopping the integration when the desorption coefficient $= 0.01$ mol. ion^{-1}. It was found that 7.5 Torr l of gas were desorbed which corresponded to 77 monolayers and that 99.75% of the desorbed gas consisted of CO, the rest being H_2, CO_2 and CH_4. Such a large quantity of gas is at first surprising but may be better understood if it is realised that the real surface area seen by the adsorbed gas - the socalled roughness factor - may be as high as 15 for our 316 L + N stainless steel[18]. After an ion dose of 1.5×10^{17} ions cm^{-2}, the discharge and the bakeout were stopped. The test chamber was demounted and stored in air in the laboratory for 4 weeks, then remounted in the analysis equipment. The result of a second argon discharge at 300°C is shown in Figure 13. Again

CO and H_2 were desorbed but in much smaller quantities. The peak ΔP was ~ 2×10^{-4} Torr and only 1.1×10^{-4} Torr l were desorbed in total. Even after several exposures to air followed by 300°C bakeouts, the recontamination level was always of the same order as that shown in Figure 14.

Pure argon discharge induced desorption from Ti and Al chambers gave essentially the same results as those obtained for stainless steel. The main component desorbed was again CO followed by H_2, CO_2 and CH_4 in essentially similar quantities as found on stainless steel.

To reduce the thermal outgassing of implanted argon the temperature of the argon discharge cleaned 316 L + N stainless steel vacuum chambers is raised from 300°C (the temperature at which the discharge is carried out) to 350°C (if of course the chamber design permits) for about 10 hours. The argon thermal degassing rate at 300°C just after discharge was 9.0×10^{-12} Torr ls^{-1} cm^{-2}, 1.2×10^{-13} Torr ls^{-1} at 300°C but after 10 hours at 350°C and $< 1 \times 10^{-15}$ Torr ls^{-1} cm^{-2} at room temperature after 10 hours at 350°C.

The effect on the desorption coefficients η of an in situ pure argon discharge in an unbaked system on a stainless steel sample is shown in Figure 15[19]. The argon discharge reduced η_{H_2}, η_{CH_4}, η_{CO} and η_{CO_2} to less than 0.01 mol. ion^{-1} but left an η_{Ar} = 0.1 mol. ion^{-1}. An argon ion dose ~ 8.3×10^{17} ions cm^{-2} was required. Under electron impact all desorption coefficients including argon were < 0.001 mol. $electron^{-1}$.

An in situ pure N_2 discharge in an unbaked system proved unsuccessful with η for mass 28 (CO and N_2) of the order of 2 to 3 mol. ion^{-1} for Ti, Al and 316 L + N stainless steel even after an ion dose of 1.6×10^{18} ions cm^{-2} but nevertheless reduced η_{H_2}, η_{CH_4} and η_{CO_2} to below 0.01 mol. ion^{-1}. As shown in Figure 16 for 316 L + N stainless steel, a subsequent pure argon discharge reduced the mass 28 desorption coefficient but left each sample with an η_{Ar} between 0.15 and 0.4 mol. ion^{-1}.

Analysis of a N_2 discharged 316 L + N stainless steel specimen produced the Auger spectra of Figure 17. A large surface concentration of N_2 was revealed (~ 45 at.%) which was certainly the source of the mass 28 desorbed.

9. THE ELECTRON POSITRON ACCUMULATOR

The CERN Electron Positron Accumulator (EPA) with a circumference of ~ 126 m has a 316 L + N stainless steel vacuum chamber (Figure 18). The vacuum chamber is not baked in situ but was prepared in accordance with UHV specifications, i.e. chemically cleaned according to the method described in section 5 above[20]. Also all vacuum chambers were subjected to a 950°C, 2 hour vacuum degassing treatment before installation. In addition, all vacuum chambers in one of the four arcs were argon glow discharge cleaned at 300°C followed by a 350°C vacuum bakeout to degas any implanted argon before installation. Thus the effects of the vacuum degassing treatment and the glow discharge cleaning on the vacuum behaviour with synchrotron radiaion could be compared.

In the EPA machine an average pressure of 7.5×10^{-10} Torr was obtained in the arcs which had been only vacuum degassed and 3.7×10^{-10} Torr in the glow discharge cleaned sector. It must be emphasised that the machine was not baked and is only pumped by sputter ion pumps whose pumping speed at these pressures is falling rapidly.

When in operation there was a marked difference between the two parts of the machine. In Figures 19a and 19b are shown the residual gas spectra from the non glow discharge cleaned and glow discharge cleaned sectors respectively.

In the vacuum degassed sector the synchrotron radiation desorbs mainly H_2 (~ 80%), CO (~ 17%) and traces of CH_4 and CO_2. On the other hand the argon glow discharge cleaning reduces markedly the CH_4 and CO_2 desorption.

10. CLEANING OF ALUMINIUM

The European Organization for Nuclear Research (CERN) is currently constructing a large electron positron storage ring (LEP) in which the average pressure over the 27 km circumference must be such that up to 6 mA of electrons and positrons may be stored for the order of 20 hours without undue loss from beam residual gas interactions. When in operation, the

inner surface of the Al alloy vacuum chamber is subjected to an intense flux of synchrotron radiation. This radiation, with a power of up to a few kW per metre, is emitted by the circulating relativistic (up to 55 GeV in the first stage of operation) electrons and positronsin the arcs of the machine. The energetic photons and the resulting photoelectrons desorb neutral gas from the vacuum chamber walls providing a large dynamic gas load which must be kept below certain limits consistent with the required beam lifetime.

One criterion therefore, for the choice of the chemical precleaning method for the vacuum chambers is that it leaves the aluminium surface with as little desorbable gas as possible.

We have compared three chemical precleaning methods suitable for aluminium alloy vacuum chambers. The methods range from vapour degreasing with no chemical attack (A), to light alkaline etching (B), and strong alkaline etching in NaOH (C).

The methods used to compare the chemical pretreatments included Auger electron spectroscopy for chemical analysis of the surface and near surface, thermal outgassing, electron and X-ray induced neutral gas desorption, measurement of the quantity of desorbed surface gas by argon glow discharge and SEM photos of the surface.

10.1 Cleaning methods

A) 1. Degreasing in perchloroethylene vapour at 121°C.

B) 1. Degreasing in perchloroethylene vapour at 121°C.

2. Immersion in alkaline (pH = 9.7) detergent at 66°C with ultrasonic agitation for 10 minutes. (The detergent is ALMECO 18 a product of Henkel and is made up to a concentration of 20 g per litre of water).

3. Rinsing in cold demineralized water.

4. Drying in a hot air oven at 150°C.

C) 1. Immersion in NaOH (concentration 45 gl^{-1}) at 45°C for one to two minutes.

2. Rinsing in demineralised water.

3. Immersion in an acid bath containing HNO_3 (concentration 50% by volume) and HF (contentration 3% by volume).

4. Rinsing in demineralised water.

5. Drying.

10.2 Auger analysis

The Auger spectra of aluminium surfaces cleaned by the three methods are shown in Fig. 20.

Degreasing in perchloroethylene vapour (A) leaves the aluminium alloy surface contaminated mainly with carbon (~47%) in the form of graphite. Other surface impurities include K, Ca, S, N and Fe (each ~ 1%). Peaks corresponding to the oxides of aluminium and magnesium are also evident. Since the magnesium oxide forms only a very thin surface layer its presence indicates no chemical attack as expected.

Cleaning with the alkaline detergent (B) results in a surface which has been lightly attacked. The outer layers containing the magnesium oxide and the trace impurities have been removed. Carbon is still the principal impurity but is much reduced (29%). The low energy aluminium oxide peak at 55 eV is evident indicating little overlying material. However, traces of phosphorous are seen presumably from the detergent which contains phosphates.

The hard etch in the NaOH solution (C) gave the best result with the lowest concentration of carbon (26%). However some fluorine (~2,5%) and copper (~0,5%) were detected. The fluorine comes from the cleaning solutions which contain it in the form of HF but the Cu is an impurity from the rinsing of a copper object in the demineralised water baths.

10.3 Auger depth profiles

As shown in Fig. 21, after perchloroethylene vapour degreasing (A), a depth profile reveals a relatively thick (~ 300 to 350 Å) oxide layer and contaminants which are still visible even after most of the oxide has been removed.

The alkaline detergent treatment (B) leaves the surface with a much reduced oxide layer thickness ~ 125 to 150 Å. The P impurity disappears after ~30 Å.

The NaOH etched surface (C) has a depth profile in which the oxygen content at first drops quickly with distance into the metal. However this decrease flattens out and the reduction in oxygen content is less abrupt than in samples cleaned by the alkaline detergent.

10.4 Thermal outgassing

The time dependance of the thermal outgassing rates for H_2, CH_4, CO, H_2O and CO_2 was measured before and after baking at 150°C for 24 hours for the three chemical treatments and the results are shown in Figs. 22 and 23.

Before bakeout it can be seen that, irrespective of the chemical treatment, the dominant outgassing species are H_2 and H_2O followed by CO then CO_2 and CH_4. Even after 120 hours of pumping the outgassing rates are still decreasing with the H_2 and the H_2O rates showing a tendency to level off.

After baking at 150° for 24 hours and after pumping for 120 hours at ambient temperature the H_2O degassing rate is $< 10^{-11}$ Pa $m^3s^{-1}m^{-2}$ and the H_2 outgassing rate dominates for all three treatments. The H_2 outgassing rate is highest in the case of the perchloroethylene vapour cleaned sample being about 2×10^{-9} Pa $m^3s^{-1}m^{-2}$ and for the other two cleaning methods each being about 1×10^{-9} Pa $m^3s^{-1}m^{-2}$.

The greatest difference is seen in the outgassing rate of the carbon based species CH_4, CO and CO_2.

In the case of the perchloroethylene vapour degreased sample both the CO_2 and CH_4 outgassing rates are less than 10^{-11} Pa $m^3s^{-1}m^{-2}$ after 120 hours with the CO showing a tendency to level off. For the alkaline detergent treatments the CO and CO_2 outgassing rates have decreased to less than 10^{-11} Pa $m^3s^{-1}m^{-2}$ after about 90 hours and 70 hours pumping respectively.

The NaOH etched sample gives even better results with CO outgassing rate going below 10^{-11} Pa $m^3s^{-1}m^{-2}$ after 80 hours and the CO_2 rate already below this level at about 40 hours.

10.5 Electron induced desorption

The method of measuring the electron induced neutral gas desorption coefficients (η) has already been described in a previous publication[4]. In brief, a W filament with one side grounded provides up to a few mA of electrons. A suitable positive bias - in this case 300 V - applied to the specimen determines the electron energy and ensures that all electrons leaving the filament are incident on the sample. A calibrated vacuum gauge, residual gas analyser and pumping orifice enables the identity and quantity of the desorbed neutral gas species to be determined.

Three samples were mounted in the machine. One sample had been subjected to treatment A, one to B and one to C. A measurement of η was made on the three samples. The system containing the samples was then baked at 150° for 24 hours and another measurement of η made. To get some idea of the spread in the results, this procedure was repeated three times with new specimens each time.

The results are shown in Fig. 24. Only H_2, CH_4, CO and CO_2 were desorbed. The vertical bars give the spread in the three η values for each gas before and after bakeout. It can be seen that a spread of as much as a factor of two is observed.

In electron and positron storage rings the composition and pressure of the residual gas are two of the main vacuum dependent parameters limiting the lifetime of the stored beam. The beam lifetime is determined mainly by

Bremsstrahlung interactions of the stored electrons or positrons with the nuclei of the residual gas. The lifetime τ depends directly on the radiation length X_o and inversely on the molecular weight M, i.e. X_o/M. The radiation length $X_o(gcm^{-2})$ for H_2, CH_4, CO and CO_2 do not vary greatly, being 58, 45.5, 37.3 and 36.1 gcm^{-2} respectively, thus the molecular weight M is the determining factor. In order to compare the three cleaning methods, we have scaled the average of the three η measurements by multiplying by the appropriate factor M/X_o, then added these four scaled η's to give a total effective η and these are the open circules in the figures.

Taking these effective η's as the criterion of cleaniness the best treatment is C followed by B then A both before and after bakeout.

For all three treatments the bakeout at 150°C for 24 hours reduces the initial η values by a factor of about 1.5.

10.6 X-ray induced desorption

The experimental equipment has already been described elsewhere[21]. Essentially X-rays from a conventional Au cathode tube operating between 20 and 80 kV could be introduced into a test vacuum chamber via a 25 μ aluminium window. Using a calibrated vacuum gauge, residual gas analyser and pumping orifice the amount and identity of the desorbed neutral gas species could be determined and the relative efficiences of the different chemical treatments compared before and after baking at 150°C for 24 hours.

In Figs. 25 and 26 are shown the desorbed fluxes in Pa m^3s^{-1} per mA of X-ray tube before and after bakeout. Again only H_2, CH_4, CO and CO_2 were desorbed. Hydrogen has the largest desorption flux followed by CO_2, CO and CH_4.

Again for comparison and using our criterion of cleanliness as defined in section 6 we have scaled each measurement by the appropriate M/X_o factor and added the four values. The results are shown by the open circles.

Cleaning methods B and C were found to almost equally effective both before and after bakeout with treatment A worst.

10.7 Glow discharge cleaning

During routine argon glow discharge cleaning of stainless steel vacuum chambers it was observed that on initiation of the discharge a large increase in pressure was produced[17]. This is tightly bound surface gas which was desorbed under the energetic argon ion bombardment. By installation of a calibrated vacuum gauge, residual gas analyser and known pumping speed the composition of the pressure pump could be determined. In addition with the help of a minicomputer the partial pressure of each desorbed species could be measured as a function of time and, by integration, the total quantity of each gas desorbed could be determined[22]. The discharge was carried out at 150°C.

This measurement can be used as a suitable criterion for the efficiency of the cleaning methods in that the best cleaning method is that which gives the least amount of desorbed gas i.e. leaves the surface with as little gas as possible.

After treatment A - the perchloroethylene vapour degreasing - the resulting pressure increase was so large and the discharge so unstable that a reliable measurement was not possible.

The results for the other two treatments are shown in Fig. 27. There it can be seen that it is mainly H_2 and CO that are left on the surface with the quantities of CO_2 and CH_4 between 2 and 3 orders of magnitude lower. In monolayers, treatment B leaves about 20 monolayers of CO and H_2 on the surface while treatment C leaves about 6 monolayers of H_2 and 1 monolayer CO. Of the two treatments tested, C was better than B.

10.8 Scanning electron micrographs

In Fig. 28 are shown scanning electron micrographs of the Al alloy surface after the three treatments.

Treatments A and B leave the surface relatively untouched but treatment C created a surface rough on the 10 μ scale with lots of holes in the submicron range. The impression is that of a sponge-like surface which, intuitively, is felt to be bad for vacuum in that the small crevices may contain contamination and cleaning solutions difficult to remove.

10.9 Conclusion

Seen by Auger electron spectroscopy the NaOH hard etch (C) gave the cleanest surface i.e. least amount of carbon and the thinnest oxide layer.

Before and after bakeout at 150^0C for 24 hours the NaOH treatment gave the lowest outgassing rates for the carbon based species CH_4, CO and CO_2. The H_2 outgassing rate was also the lowest but the difference between the three treatments was less marked.

The difference between the worst treatment, A, and the best, C, as seen by electron induced gas desorption, was less than a factor of two, both before and after bakeout.

The X-ray induced desorption showed that, before and after bakeout, treatment A was worst with little to choose between treatments B and C.

The greatest difference between treatments B and C was seen when applying the technique of argon glow discharge cleaning. Compared to treatment B, treatment C left the aluminium surface with almost a factor of 3 less H_2 and a factor of 10 less CO.

The scanning electron micrographs showed that treatment C created a sponge-like surface which, contrary to expectation, gave improved vacuum characteristics.

In general, treatment C was best followed closely by B then A.

11. ACTUAL CLEANING OF LEP VACUUM CHAMBERS

Because of the complexity and cost of an installation capable of treating 12 metre long vacuum chambers in NaOH, HNO_3 with appropriate water rinsing a variant of method B was used to clean the LEP vacuum chambers. An alkaline detergent (Almeco 29) with a removal rate, at the same concentration (2%) and temperature (60°C) of about 1100 Å min^{-1}, i.e. 9 times that of Almeco 18 was sprayed inside and outside with high pressure jets (~ 100 bar). In addition, a second product (Amklene D forte) diluted to 2% with a removal rate 54 times that of Almeco 18 at 60°C was also sprayed into the vacuum chamber. Rinsing with demineralized water was also carried out with the same system. Drying was by hot air at ~ 80°C.

Two LEP vacuum chambers cleaned by this high pressure jet process by two different manufacturers were exposed to synchrotron radiation in the dedicated beam line of the synchrotron radiation source at L.U.R.E., Orsay, France and the results compared with a similar chamber which had been cleaned with method C i.e. NaOH + HNO_3.

The results are shown in Fig. 29 where instead of showing the individual gases desorbed we have calculated their effect on the beam lifetime - the important parameter which depends on the gas composition and pressure. In addition the clean-up rate in mA hours of machine operation (essentially exposure time to synchrotron radiation) is indicated.

Both chambers show, at the very first instant, higher desorption due to photon bombardment than the reference chamber cleaned by method C resulting in a factor 5 shorter lifetime. In spite of a number of differences in the manufacture and preparation of both chambers the results are in very close agreement.

The clean up with photon bombardment is very fast for both chambers and approaches or even exceeds a slope of -1 for CH_4 and CO_2. In line with previous observations CO cleans up slower than the other gas species.

A comparison, in terms of the effect of the dynamic pressure rise on beam lifetime, between the two test chambers and the reference chamber, indicates that the improvement in beam lifetime with increasing beam dose is such that the initial large difference has practically vanished after 1 Ah of machine operation.

ACKNOWLEDGEMENTS

The author is indebted to his co-workers at Orsay, his colleagues at CERN, especially those in the LEP Division Vacuum Group whose professional efforts in the field of UHV applied to large machines over many years have greatly contributed to this publication.

REFERENCES

1. C. Benvenuti, J-M. Laurent and F. Scalambrin, Proc. VIIth Int. Vac. Congress, Vienna, 113, (1977).

2. R.S. Calder, Vacuum 24, (10), 437 (1974).

3. F.G. Allen, J. Eisinger, H. Hagstrom and J.T. Law, J. Appl. Phys., 30 (10), 1563, (1959).

4. A.G. Mathewson, Vacuum 24, 505, (1974).

5. A.G. Mathewson, CERN Internal Report, CERN-ISR-VA/76-5, (1976).

6. O. Gröbner, A.G. Mathewson, H. Störi, P. Strubin and R. Souchet, Vacuum 33 (7), 397 (1983).

7. P.W. Palmberg, G.K. Bohn and J-C. Tracy, Appl. Phys. Lett. 15 (8), 254, (1969).

8. R.S. Barton and R.P. Govier, Vacuum 20, 1 (1970).

9. T.W. Haas, J.T. Grant and G.J. Dooley III, J. Appl. Phys., 43 (4), 1853 (1972).

10. P.A. Redhead, Vacuum 12, 203 (1962).

11. A.G. Mathewson, R. Calder, A. Grillot and P. Verbeeck, Proc. VIIth Int. Vac. Congress, Vienna, 1027 (1977).

12. C.J. Smithells, Metals Reference Handbook, Vol. II, Butterworths, London, 66 (1962).

13. Marie-Hélène Achard, R. Calder and A.G. Mathewson, Vacuum 29, (2) 53 (1979).

14. T.E. Madey and J.T. Yates Jr., J. Vac. Sci. Technol., 8, 525, (1971).

15. G. Carter and J.S. Colligon, 'Ion Bombardment of Solids', Elsevier Publishing Co. Inc., New York, (1968).

16. R.M. Lambert and C.M. Comrie, J. Vacuum. Sci. Technol., 11, (2), 530 (1974).

17. R. Calder, A. Grillot, F. Le Normand and A.G. Mathewson, Proc. VIIth Int. Vac. Congress, Vienna, 231 (1977).

18. K. Watanabe, S. Maeda, T. Yamashina and A.G. Mathewson, J. Nuclear Mat. 93 & 94, 679 (1980).

19. Marie-Hélène Achard, CERN Internal Report, CERN-ISR-VA/76-34, (1976).

20. A. Poncet, CERN Internal Report, CERN-PS/87-42(ML) PS/ML/Note 85-25, March 15th 1987.

21. N. Hilleret, IXth Int. Vac. Congress, Madrid (1983).

22. P. Strubin, IXth Int. Vac. Congress, Madrid (1983).

FIGURE CAPTIONS

1a) The residual gas spectrum in a baked Al vacuum chamber before exposure to synchrotron radiation.

1b) The residual gas spectrum during the metal exposure to radiation.

2) A schematic diagram of the equipment used for measuring the electron and ion induced neutral gas desorption coefficients.

3) Auger spectra of stainless steel surfaces after various stages of the chemical solvent cleaning procdure.

4) A schematic diagram of the flash desorption equipment.

5) The flash desorption spectrum of CO from non-degassed 316 L + N stainless steel.

6) The surface composition of 316 L + N stainless steel after heating to various temperatures between ambient and 900°C.

7) The percentage of C, O and S on a stainless steel surface as a function of temperature.

8) The temperature dependence of the electron and ion induced desorption coefficients for 316 L + N stainless steel.

9) The miniature stainless steel discharge cell used in conjunction with the Auger analysis system.

10) Auger spectra of 316 L + N stainless steel before and after pure argon discharge cleaning treatments.

11) Auger spectra of 316 L + N stainless steel before and after discharge cleaning with argon/10% oxygen.

12) The apparatus for analysis of the gas discharge induced pressure rises.

13) The composition and time dependence of a typical gas discharge induced pressure rise.

14) The result of a second argon discharge after exposure of the chamber to air.

15) The effect on the desorption coefficients of an in situ pure argon glow discharge in an unbaked system on a stainless steel sample.

16) The effect on the desorption coefficients of an in situ pure N_2 discharge in an unbaked system on a stainless steel sample.

17) Auger spectra of an N_2 discharged 316 L + N stainless steel specimen.

18) The CERN Electron Positron Accumulator.

19a) The residual gas spectrum in the vacuum degassed sector after 0.5 Ah of beam dose and at 65 mA of circulating beam.

19b) The residual gas spectrum in the argon glow discharged sector under the same conditions.

20) The Auger spectra of aluminium surfaces cleaned by the three cleaning methods.

21) Auger depth profiles of aluminium samples cleaned by the three cleaning methods.

22) The time dependence of the thermal outgassing rates before baking for the three cleaning methods.

23) The time dependence of the thermal outgassing rates after baking at 150°C for 24 hours for the three cleaning methods.

24) The electron induced neutral gas desorption coefficients before and after baking at 150°C for 24 hours for the three cleaning methods.

25) The X-ray induced desorbed gas flux from aluminium chambers before bakeout for the three cleaning methods.

26) The X-ray induced desorbed gas flux from aluminium chambers after bakeout at 150°C for 24 hours for the three cleaning methods.

27) The quantity of gas desorbed from an aluminium surface by an argon discharge after treatments B and C.

28) Scanning electron micrographs of the aluminium alloy surface after the three cleaning methods.

29) The beam-residual gas lifetime as a function of the accumulated beam dose for the reference chamber cleaned by method C and two other chambers cleaned by a variant of method B.

TABLE I

(seconds)

E(eV) \ T°C	200	300	400
0.9	3.8×10^{-4}	8.1×10^{-6}	5.4×10^{-7}
1.7	1.2×10^{5}	8.6×10^{1}	5.2×10^{1}
2.0	1.9×10^{8}	3.7×10^{4}	9.1×10^{1}
2.8	6.4×10^{16}	4.0×10^{11}	8.8×10^{7}

TABLE II

E(eV)

	316 L + N non-degassed	316 L + N degassed	316 L	NS 21
α-CO	0.97		1.2	≈ 0.9
β-CO	1.72	1.67	1.7	1.55
γ-CO	2.05	1.91	2.2	1.96
δ-CO (?)			2.8	
H_2				0.89

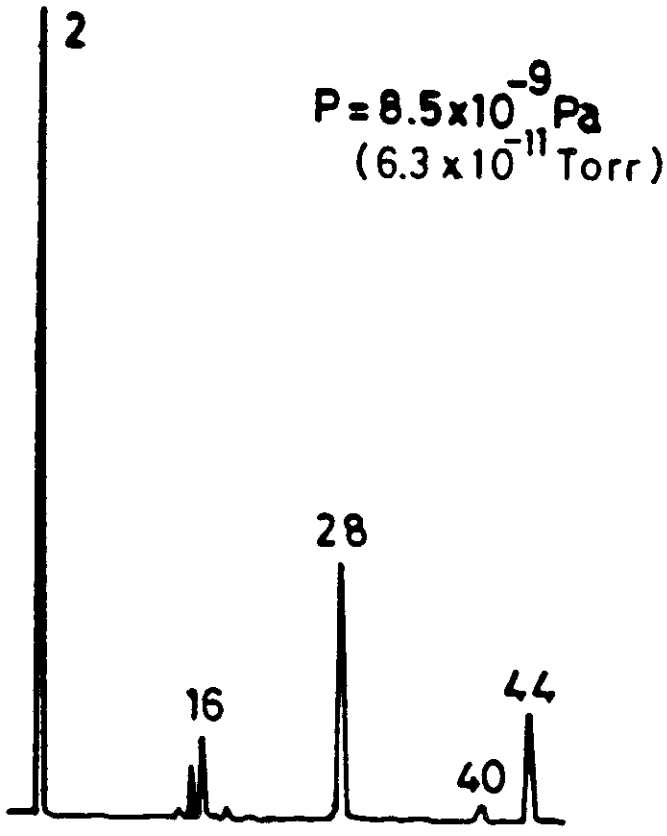

Fig. 1a : The residual gas spectrum before exposing the test chamber to synchrotron radiation

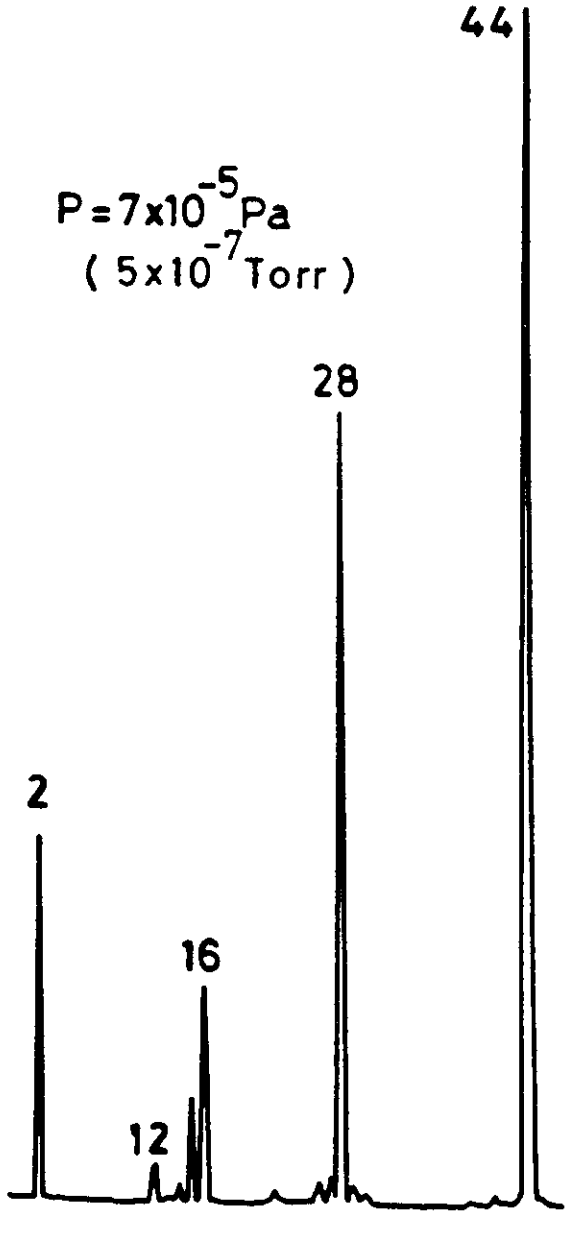

Fig. 1b : The residual gas spectrum during exposure to synchrotron radiation

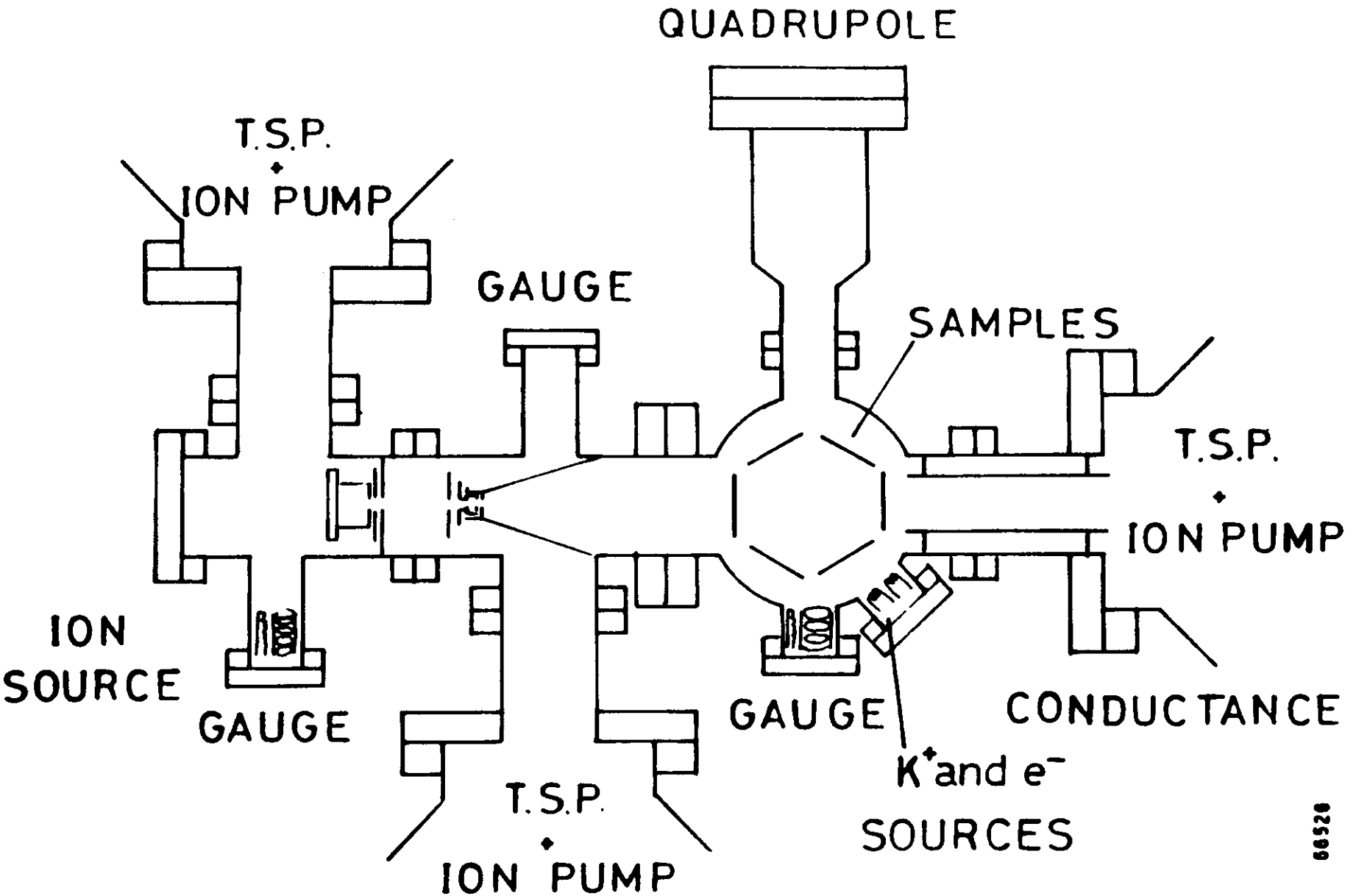
QUADRUPOLE
T.S.P.
ION PUMP
GAUGE
SAMPLES
T.S.P.
ION PUMP
ION
SOURCE
GAUGE
GAUGE
CONDUCTANCE
K+ and e-
SOURCES
T.S.P.
ION PUMP
88528

Figure 2

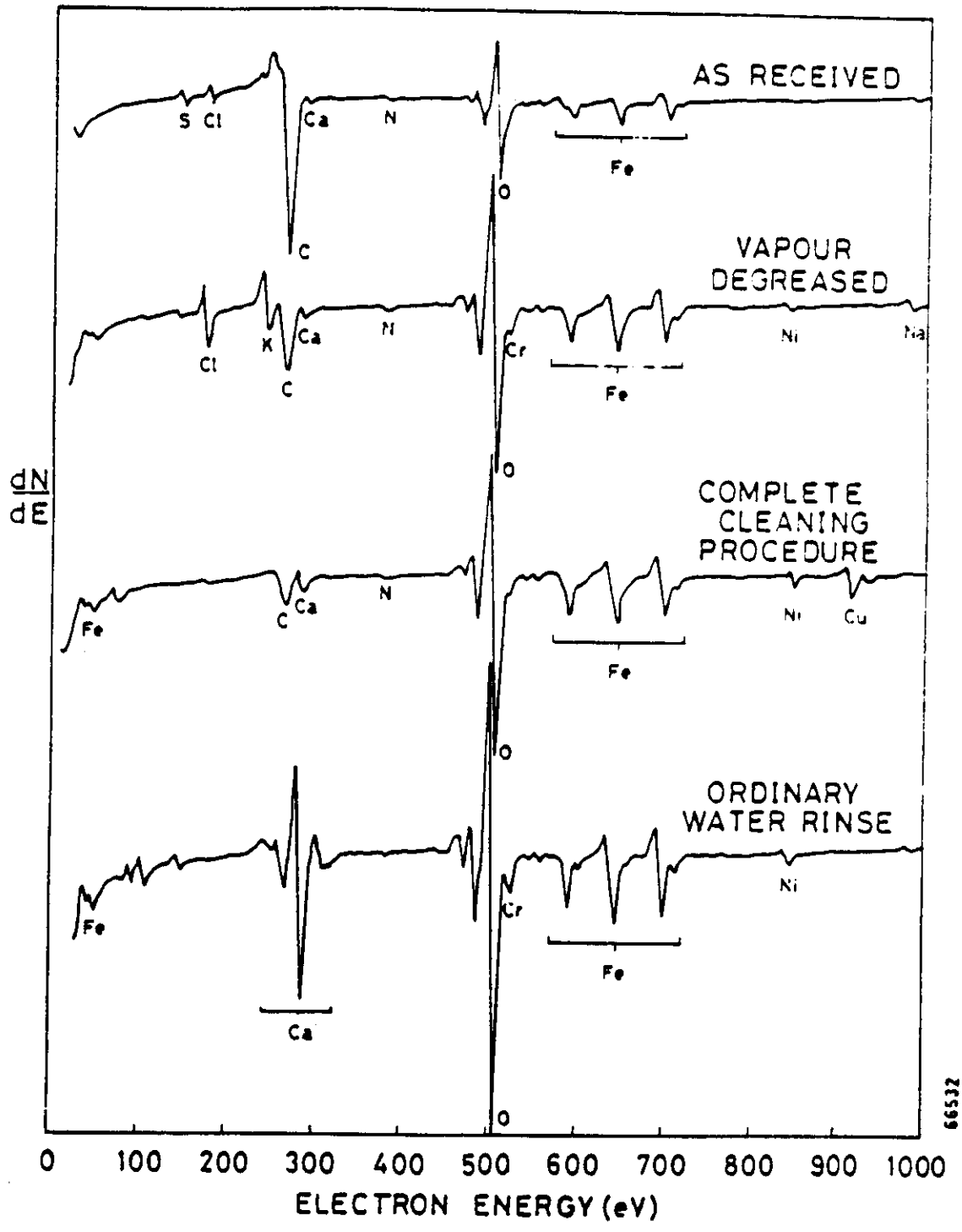
AS RECEIVED
S Cl
Ca
N
O
C
Fe
VAPOUR DEGREASED
Cl
K
Ca
C
N
Cr
Ni
Fe
COMPLETE CLEANING PROCEDURE
Fe
C
Ca
N
Ni
Cu
Fe
ORDINARY WATER RINSE
Fe
Ca
Cr
Ni
Fe
dN/dE
0
100
200
300
400
500
600
700
800
900
1000
ELECTRON ENERGY (eV)
66532

Figure 3

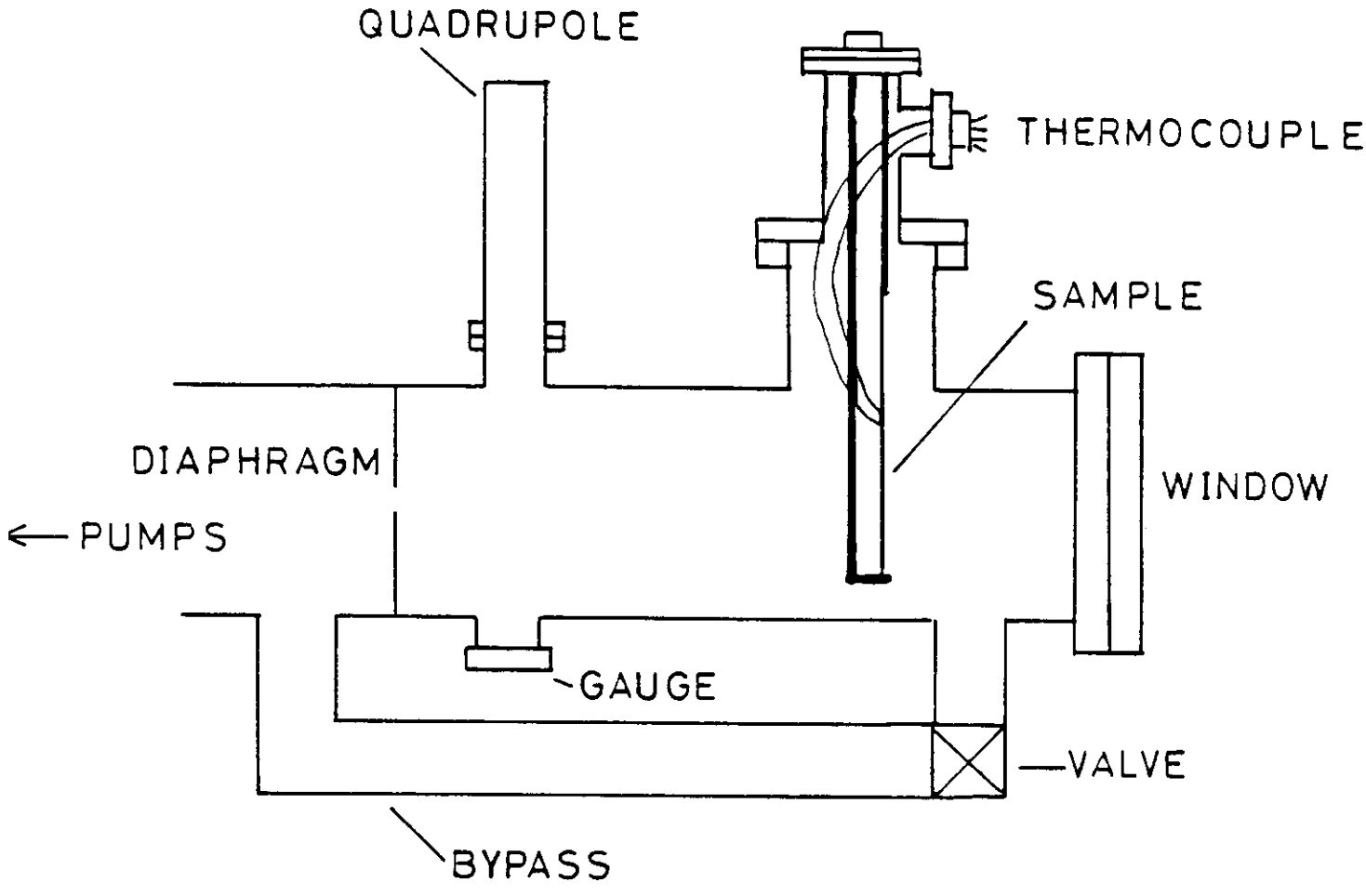
QUADRUPOLE
THERMOCOUPLE
SAMPLE
DIAPHRAGM
WINDOW
← PUMPS
GAUGE
VALVE
BYPASS

Figure 4

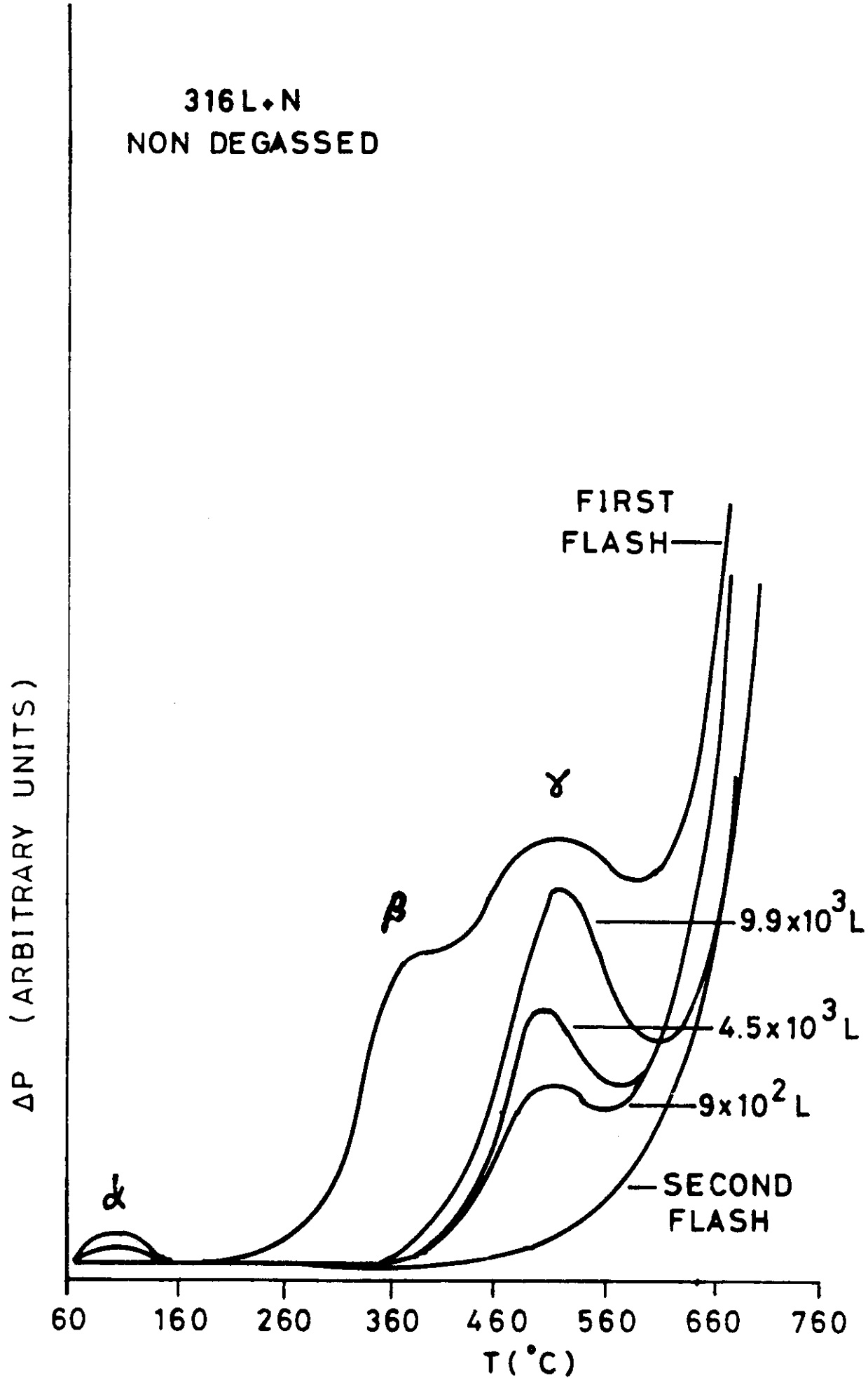
316 L • N
NON DEGASSED
FIRST
FLASH
γ
β
α
9.9x10³L
4.5x10³L
9x10²L
SECOND
FLASH
ΔP (ARBITRARY UNITS)
60
160
260
360
460
560
660
760
T(°C)

Figure 5

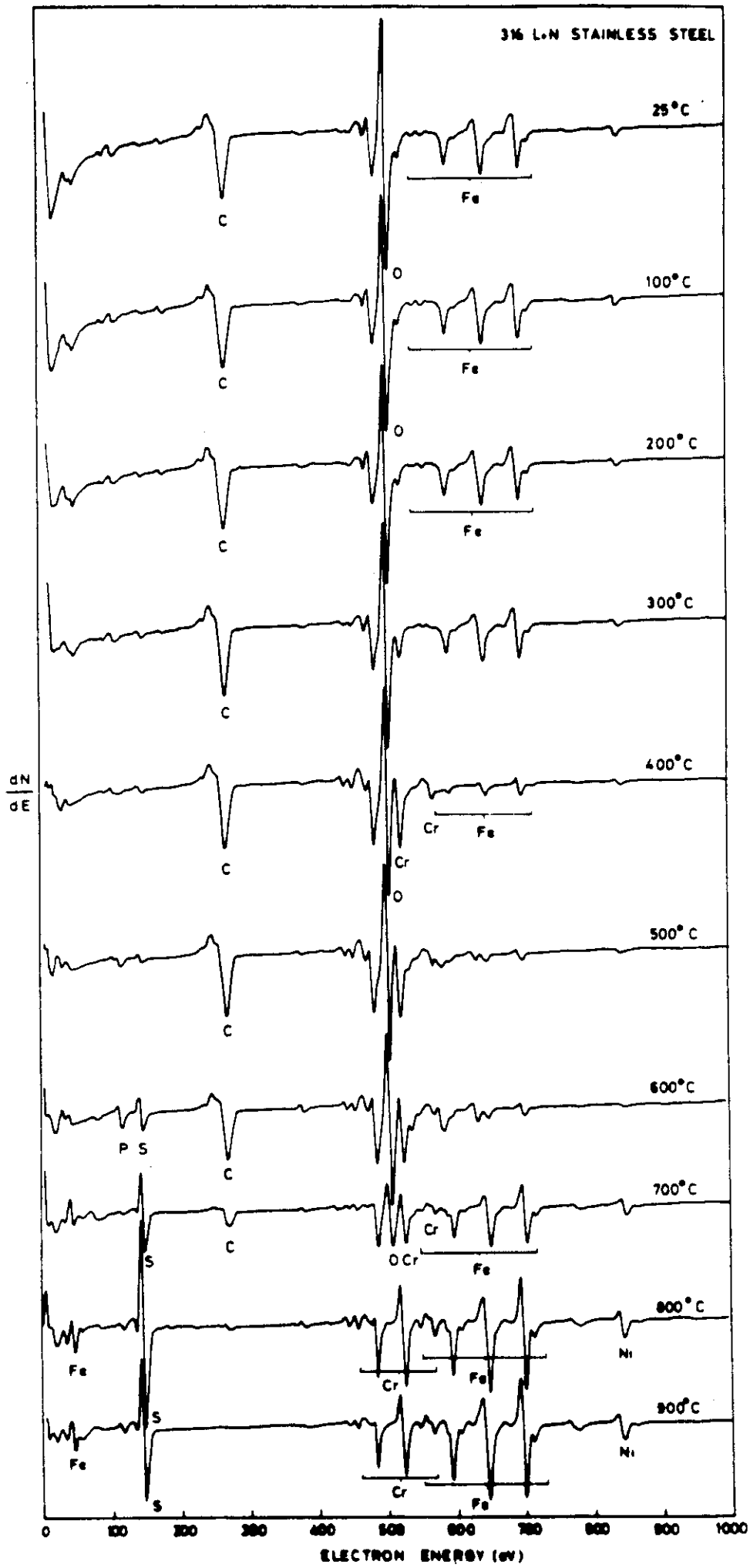
316 L-N STAINLESS STEEL
25°C
100°C
200°C
300°C
400°C
500°C
600°C
700°C
800°C
900°C
C
O
Fe
Cr
P
S
Ni
dN/dE
0
100
200
300
400
500
600
700
800
900
1000
ELECTRON ENERGY (eV)

Figure 6

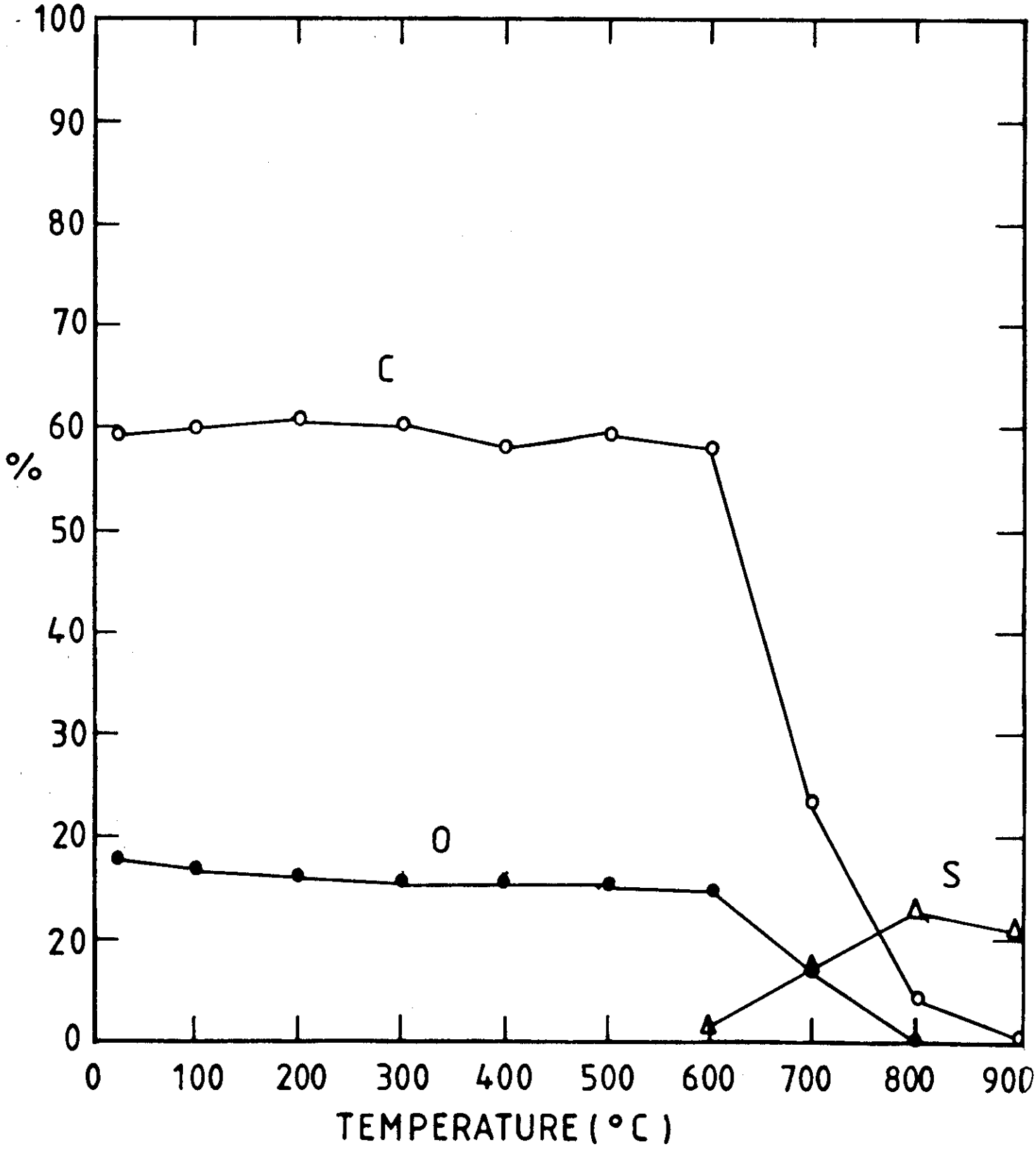
100
90
80
70
60
50
40
30
20
20
0
%
C
O
S
0
100
200
300
400
500
600
700
800
900
TEMPERATURE (°C)

Figure 7

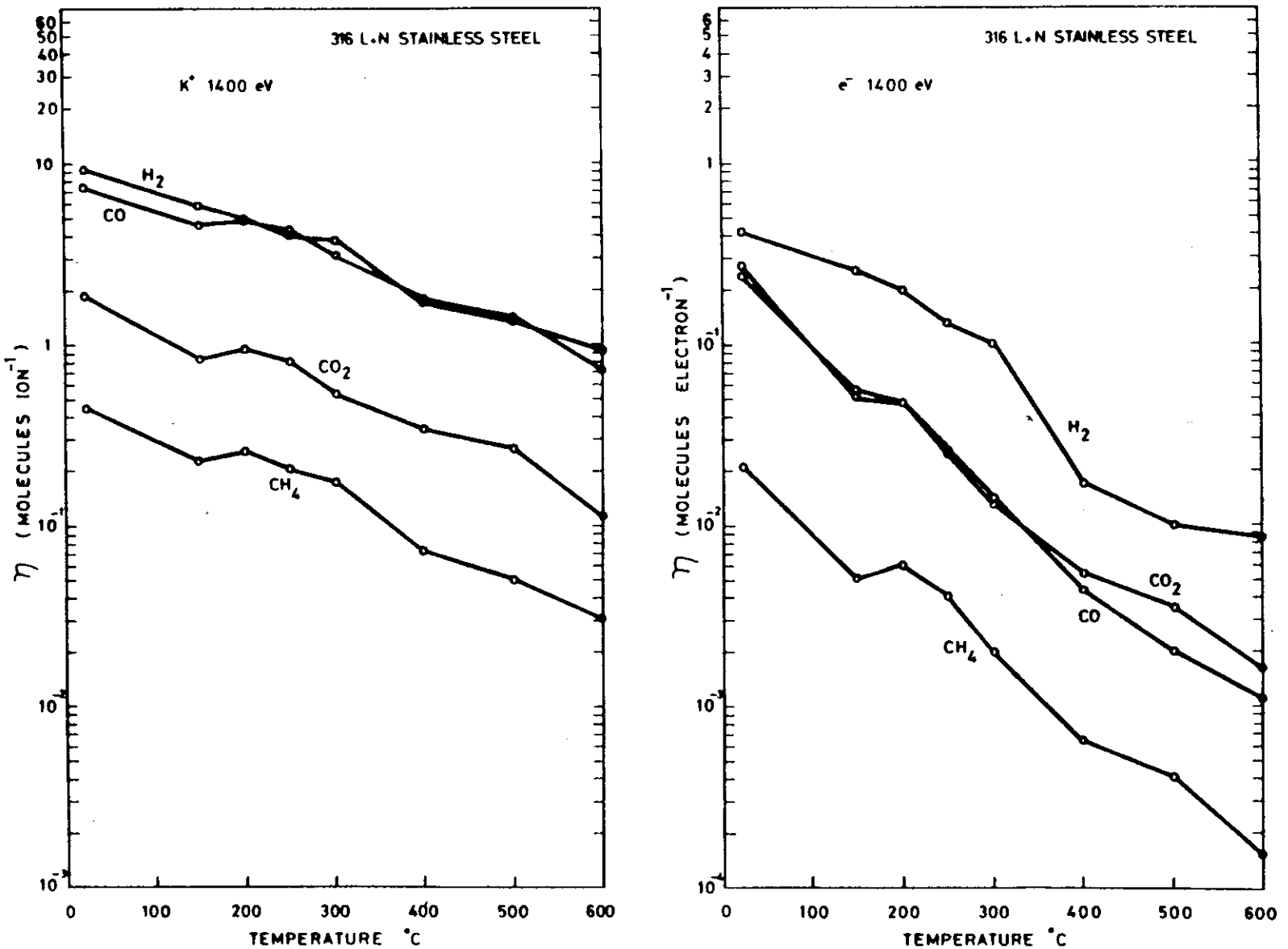
316 L.N STAINLESS STEEL
K⁺ 1400 eV
H2
CO
CO2
CH4
η (MOLECULES ION⁻¹)
TEMPERATURE °C
316 L.N STAINLESS STEEL
e⁻ 1400 eV
H2
CO2
CO
CH4
η (MOLECULES ELECTRON⁻¹)
TEMPERATURE °C

Figure 8

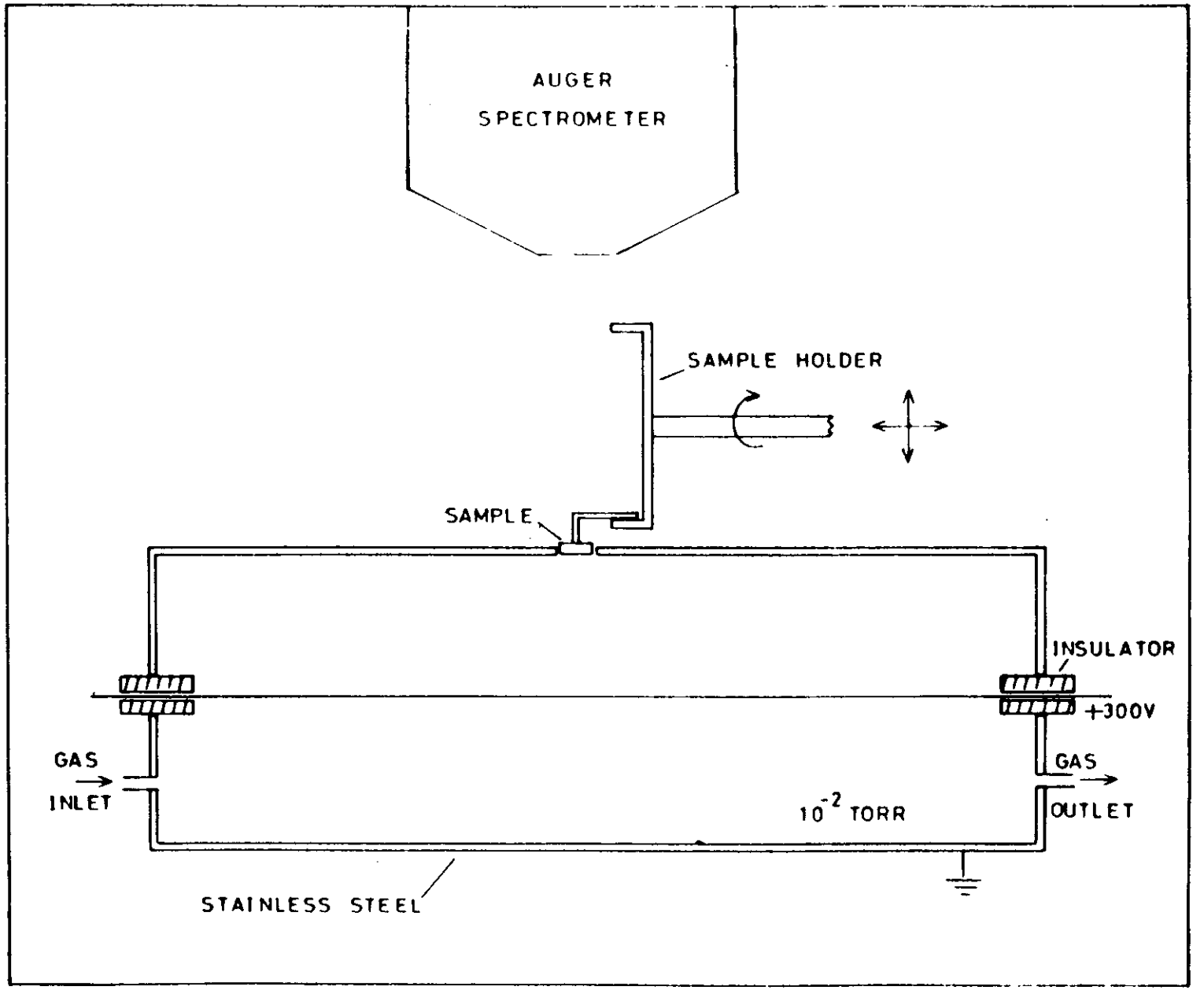
AUGER
SPECTROMETER
SAMPLE HOLDER
SAMPLE
INSULATOR
+300V
GAS
INLET
GAS
OUTLET
10^{-2} TORR
STAINLESS STEEL
66534

Figure 9

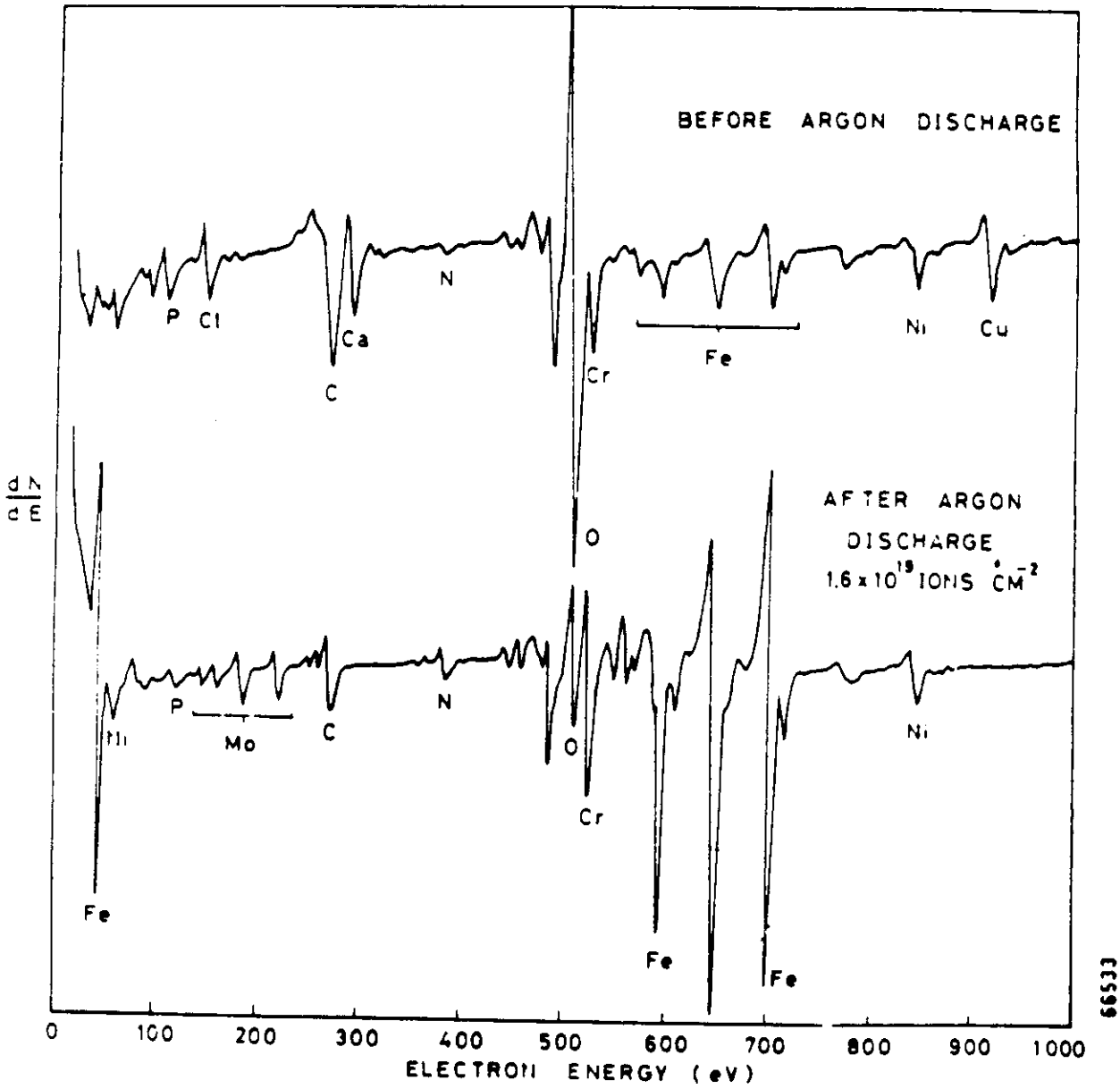
BEFORE ARGON DISCHARGE
P
Cl
Ca
C
N
O
Cr
Fe
Ni
Cu
AFTER ARGON
DISCHARGE
1.6 x 10^19 IONS CM^-2
Ti
P
Mo
C
N
O
Cr
Fe
Fe
Fe
Ni
dN/dE
0
100
200
300
400
500
600
700
800
900
1000
ELECTRON ENERGY (eV)
66533

Figure 10

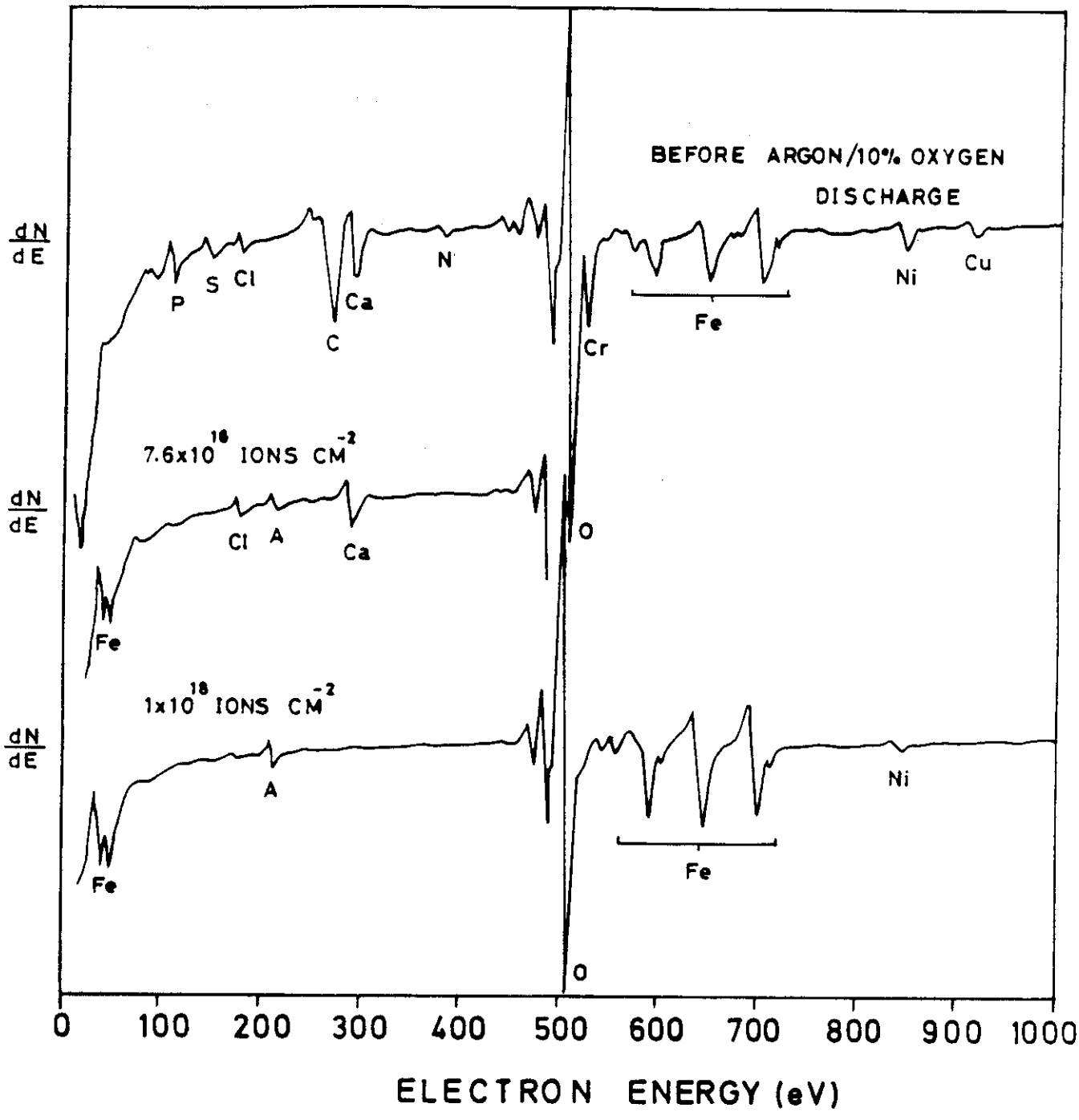
BEFORE ARGON/10% OXYGEN
DISCHARGE
dN/dE
P
S
Cl
C
Ca
N
Cr
Fe
Ni
Cu
7.6x10^16 IONS CM^-2
Cl
A
Ca
O
Fe
1x10^18 IONS CM^-2
A
Ni
Fe
O
0
100
200
300
400
500
600
700
800
900
1000
ELECTRON ENERGY (eV)

Figure 11

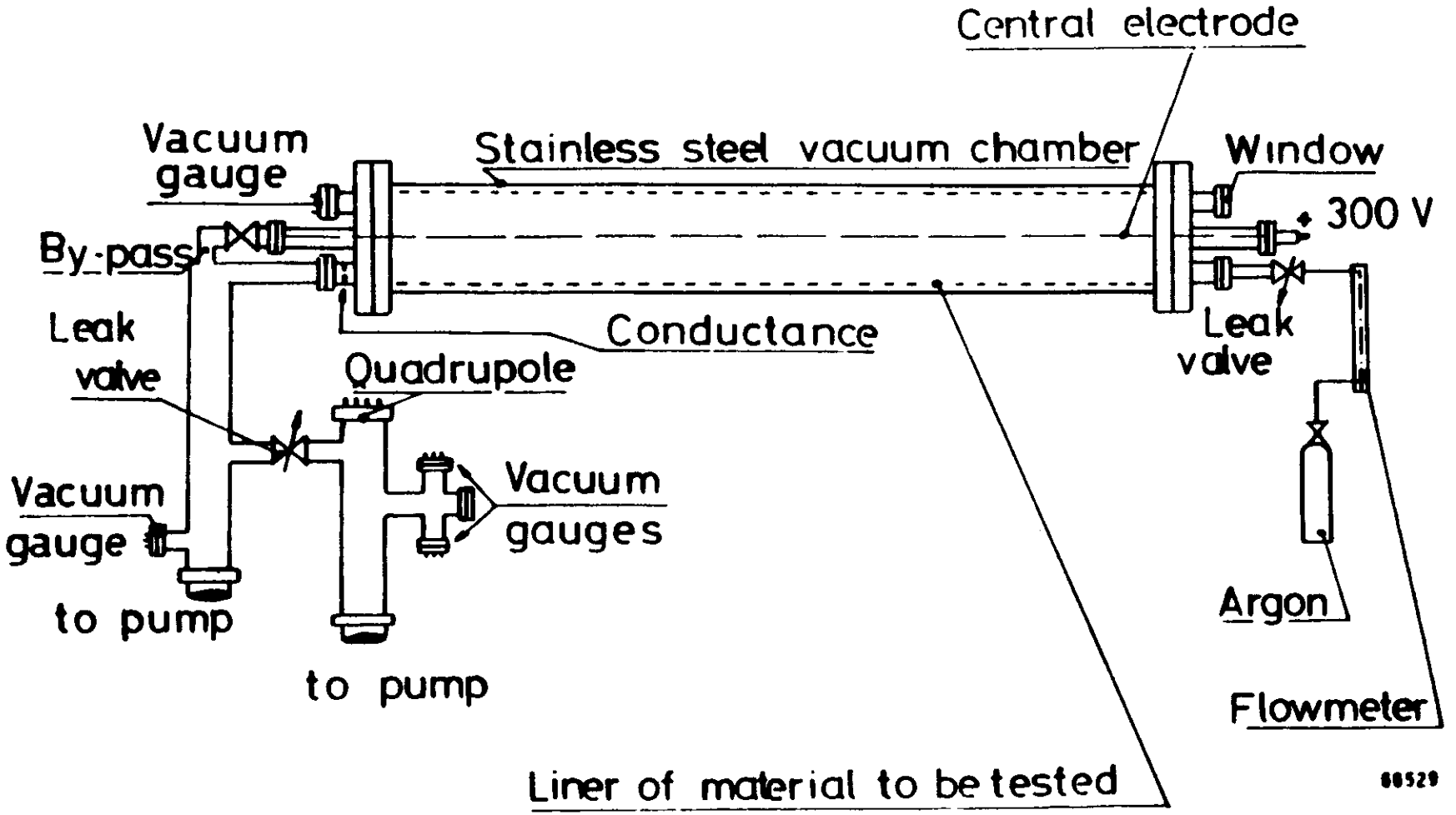
Central electrode
Vacuum gauge
Stainless steel vacuum chamber
Window
300 V
By-pass
Leak valve
Conductance
Quadrupole
Leak valve
Vacuum gauge
Vacuum gauges
to pump
to pump
Argon
Flowmeter
Liner of material to be tested
88529

Figure 12

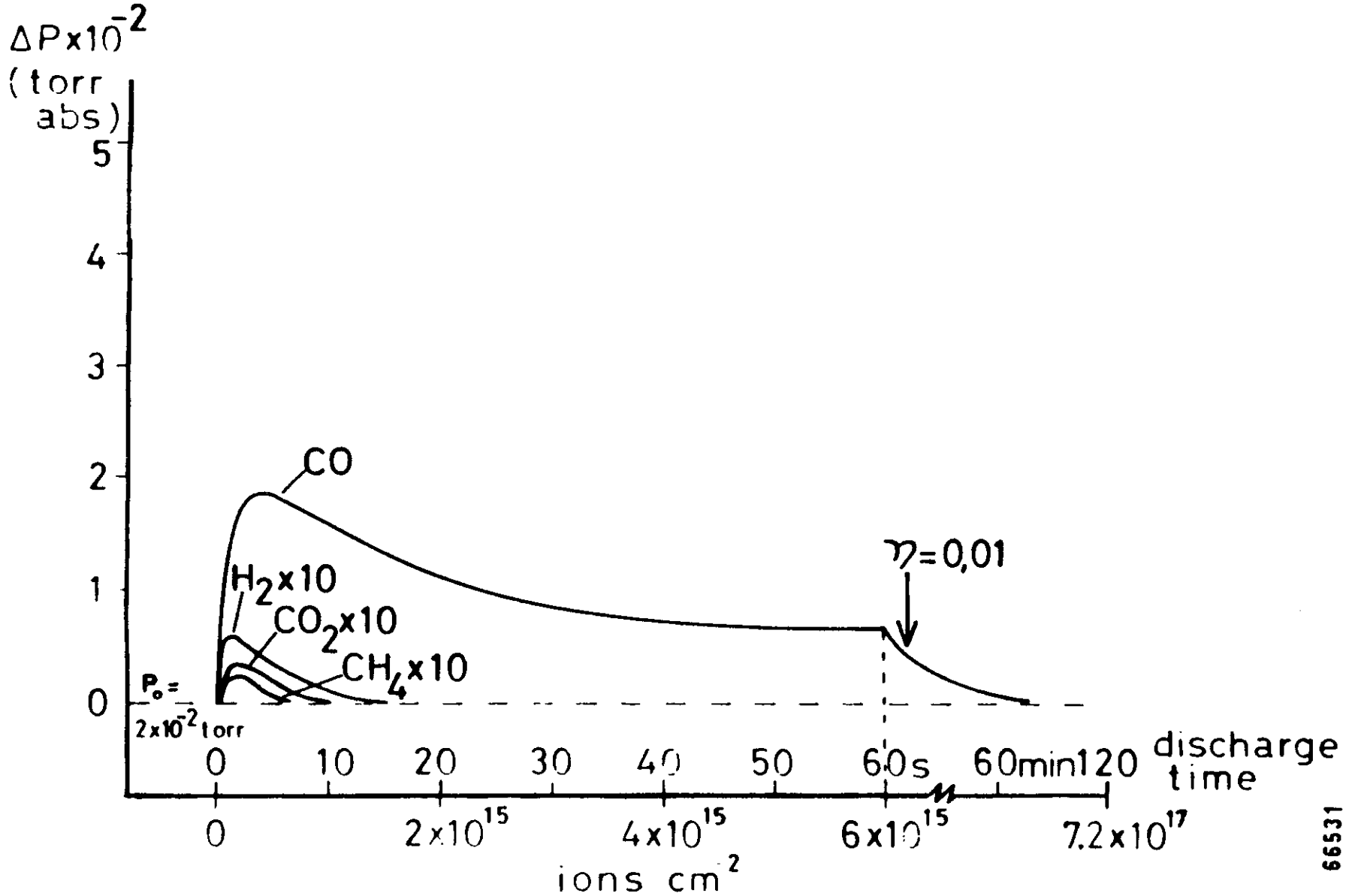
ΔPx10⁻²
(torr abs)
5
4
3
2
1
0
CO
H2x10
CO2x10
CH4x10
η=0,01
P₀ =
2x10⁻² torr
0
10
20
30
40
50
60s
60min120
discharge time
0
2x10¹⁵
4x10¹⁵
6x10¹⁵
7.2x10¹⁷
ions cm⁻²
66531

Figure 13

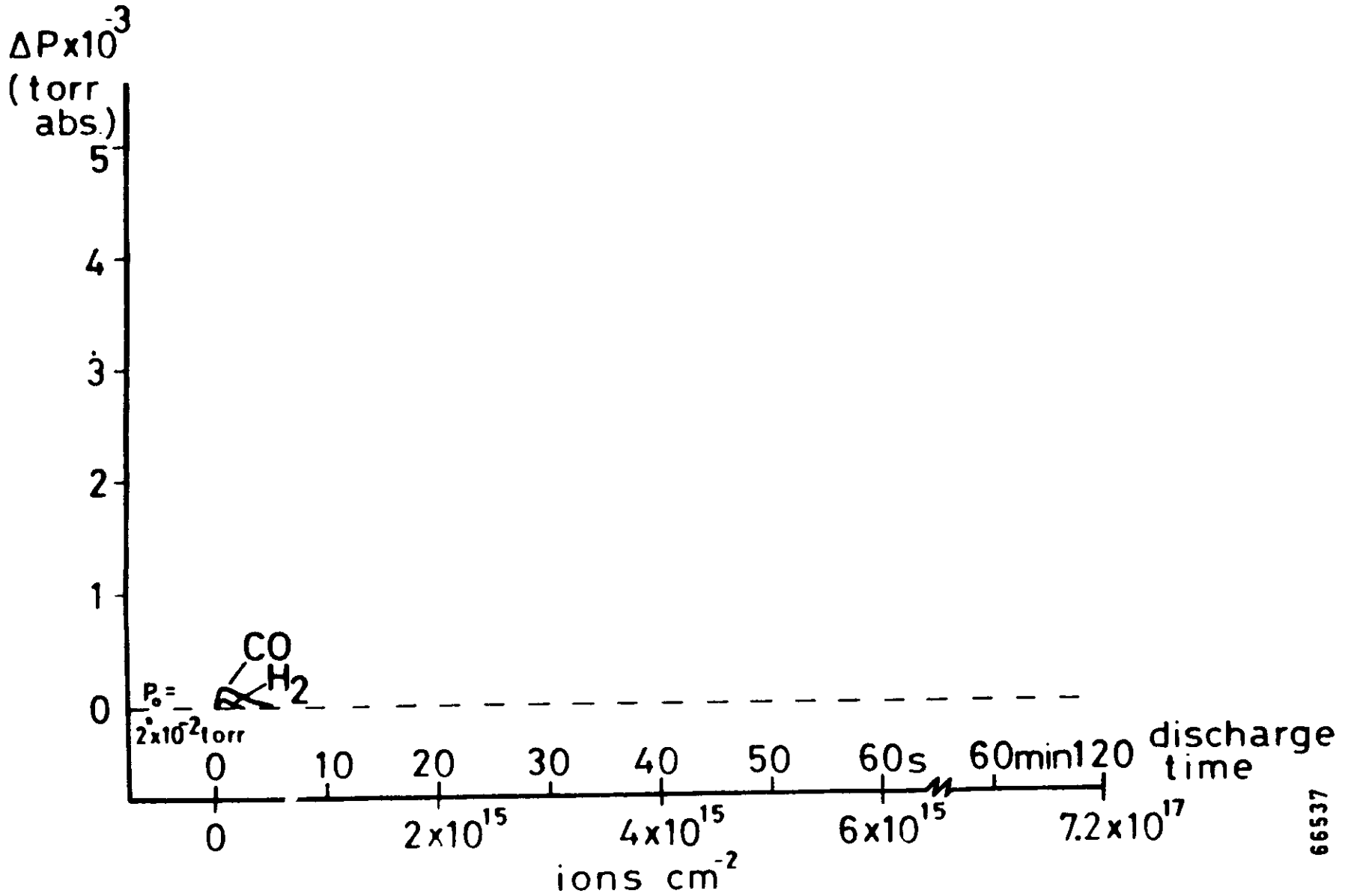
ΔPx10^-3
(torr abs.)
5
4
3
2
1
0
CO
H2
P0 = 2x10^-2 torr
0
10
20
30
40
50
60s
60min
120
discharge time
0
2x10^15
4x10^15
6x10^15
7.2x10^17
ions cm^-2
66537

Figure 14

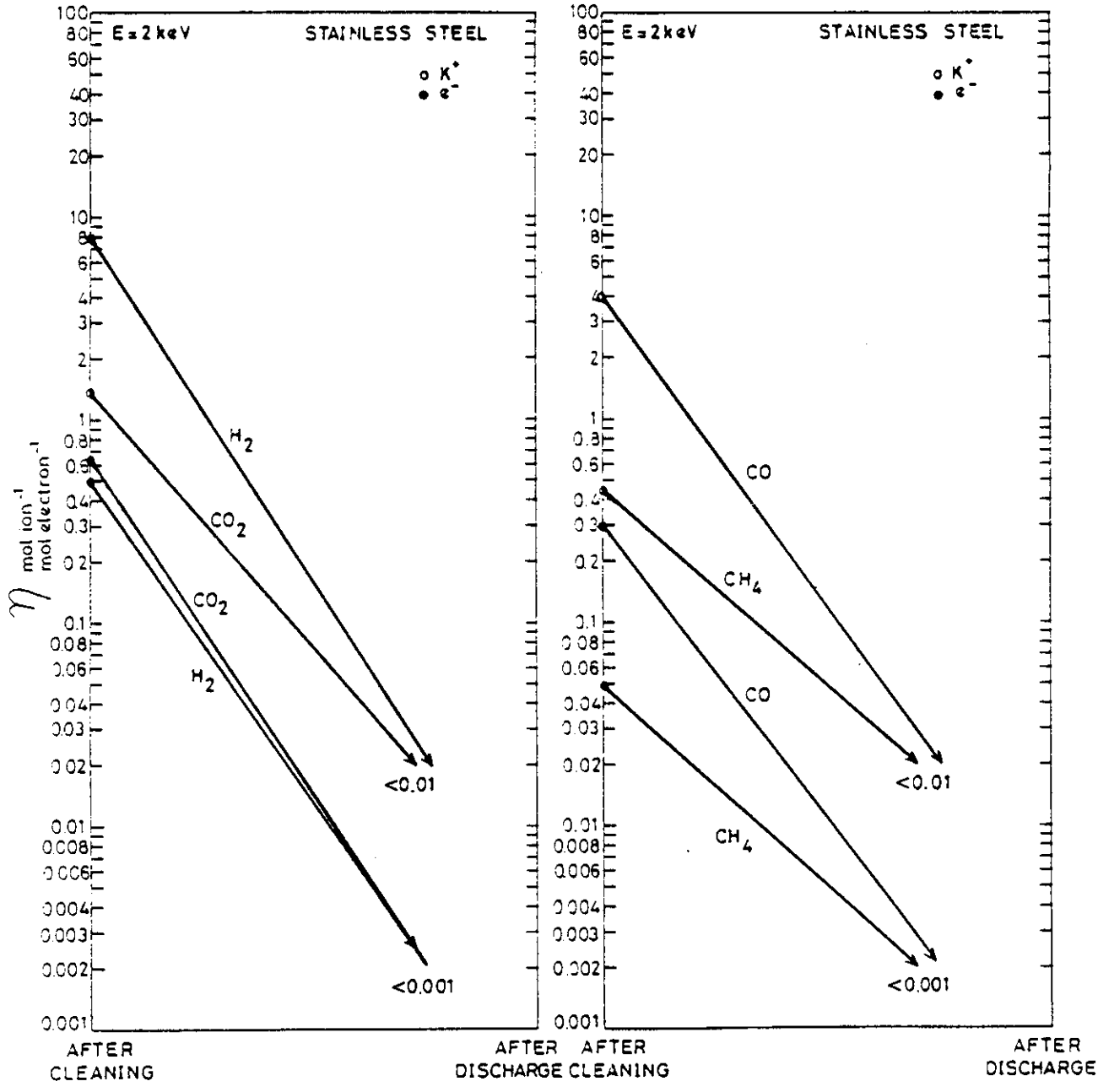
E = 2 keV
STAINLESS STEEL
o K+
• e−
η
mol ion−1
mol electron−1
H2
CO2
CO2
H2
<0.01
<0.001
AFTER CLEANING
AFTER DISCHARGE
E = 2 keV
STAINLESS STEEL
o K+
• e−
CO
CH4
CO
CH4
<0.01
<0.001
AFTER CLEANING
AFTER DISCHARGE

Figure 15

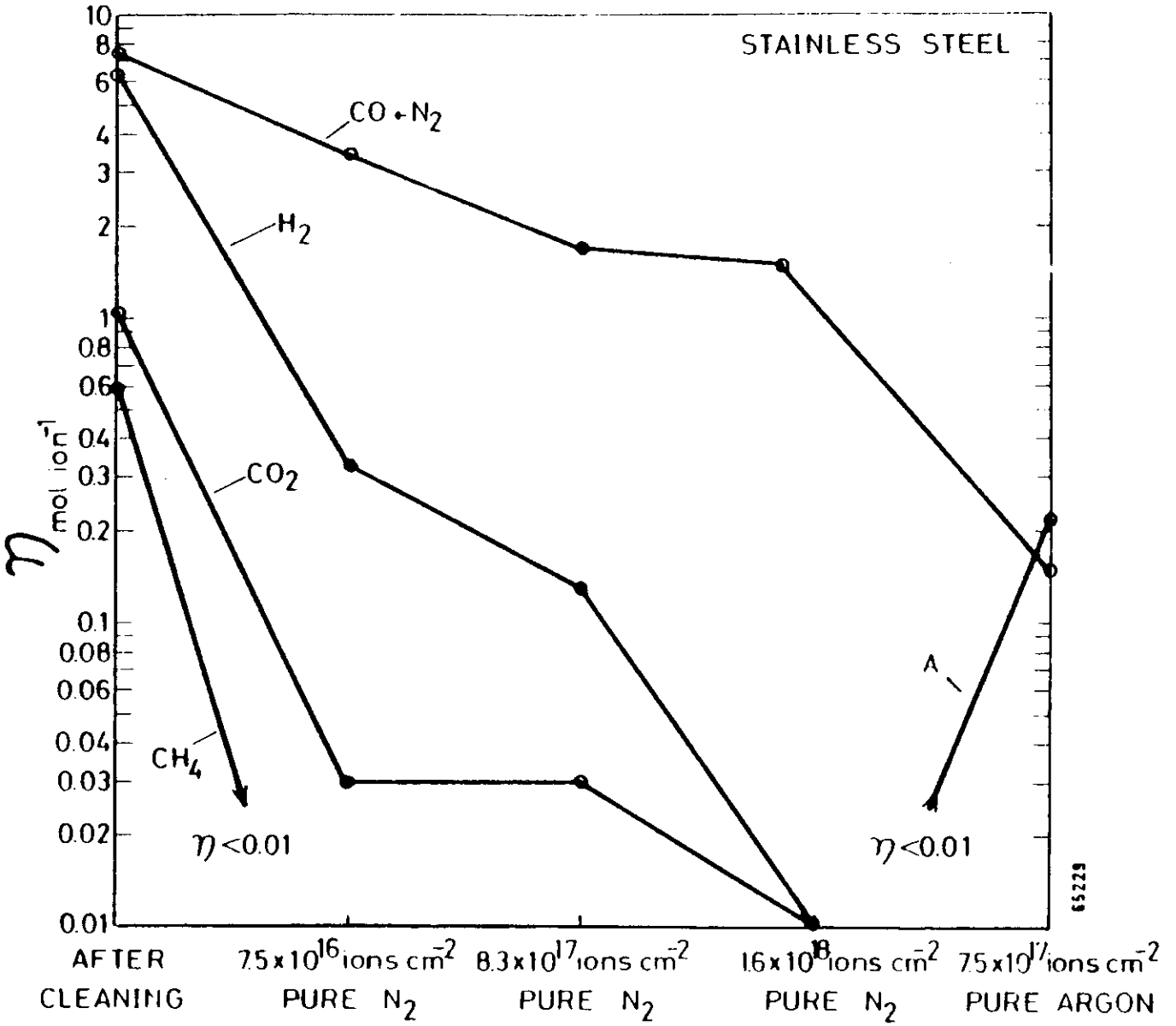
STAINLESS STEEL
CO + N2
H2
CO2
CH4
A
η <0.01
η <0.01
η mol ion-1
10
8
6
4
3
2
1
0.8
0.6
0.4
0.3
0.2
0.1
0.08
0.06
0.04
0.03
0.02
0.01
AFTER CLEANING
7.5x10^16 ions cm^-2 PURE N2
8.3x10^17 ions cm^-2 PURE N2
1.6x10^18 ions cm^-2 PURE N2
7.5x10^17 ions cm^-2 PURE ARGON
65223

Figure 16

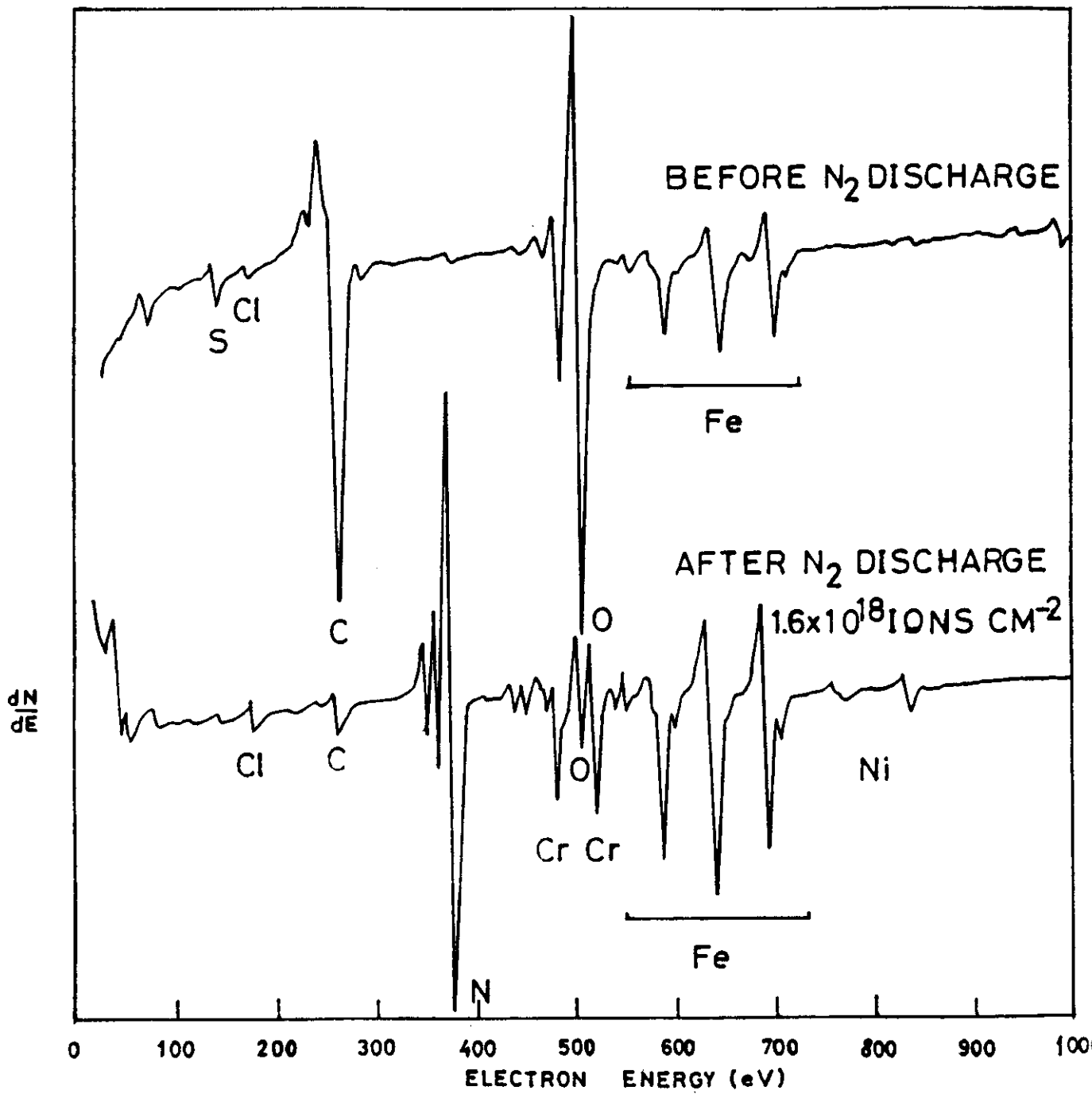
BEFORE N_2 DISCHARGE
S
Cl
Fe
AFTER N_2 DISCHARGE
1.6×10^{18} IONS CM^{-2}
C
O
Cl
C
O
Ni
Cr Cr
Fe
N
$\frac{dN}{dE}$
0
100
200
300
400
500
600
700
800
900
1000
ELECTRON ENERGY (eV)

Figure 17

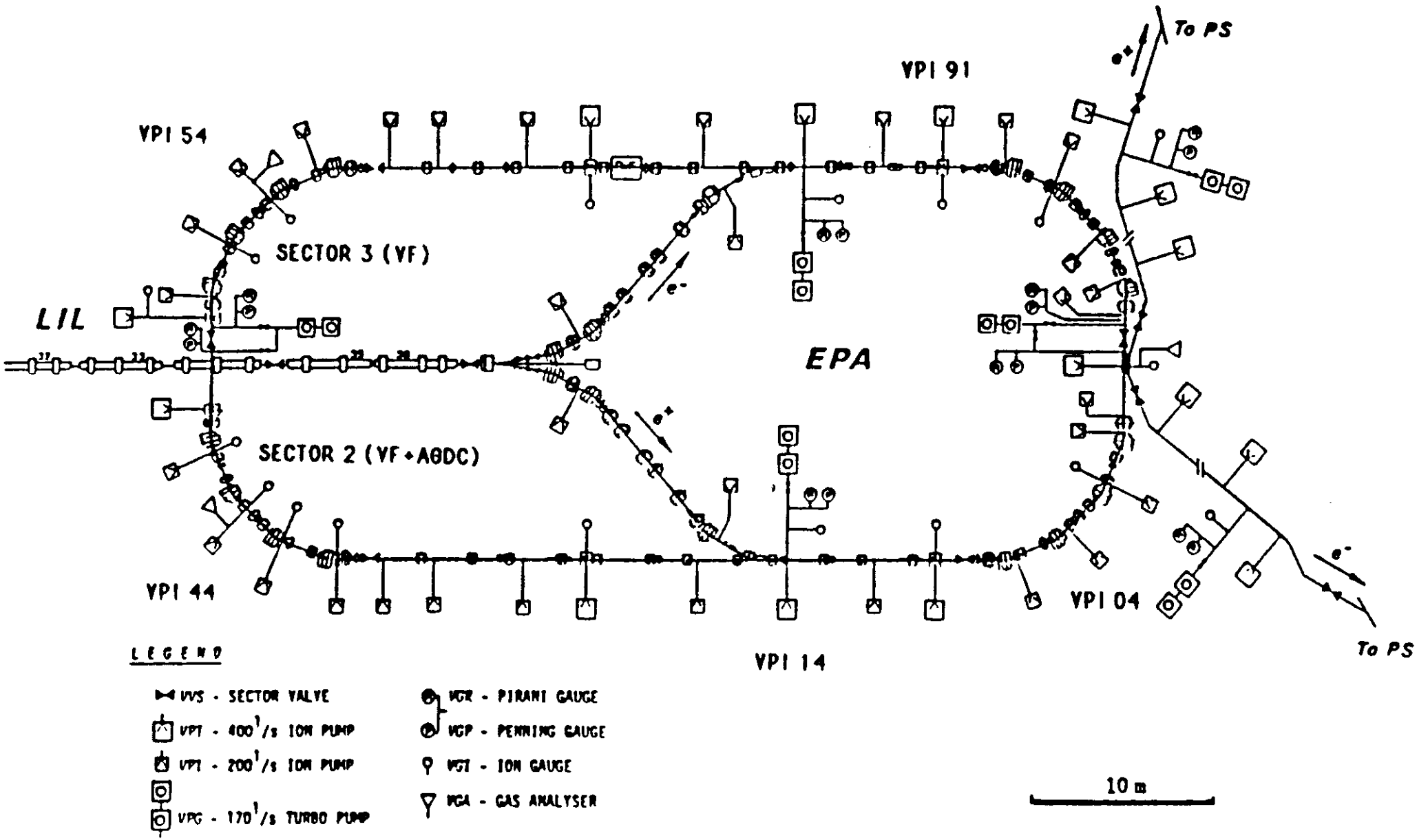

Figure 18

EPA VACUUM SYSTEM LAYOUT.

FIGURE 19a

The residual gas spectrum in the Vacuum fired pilot sector of EPA after .5Ah of beam dose and 65mA of circulating current.

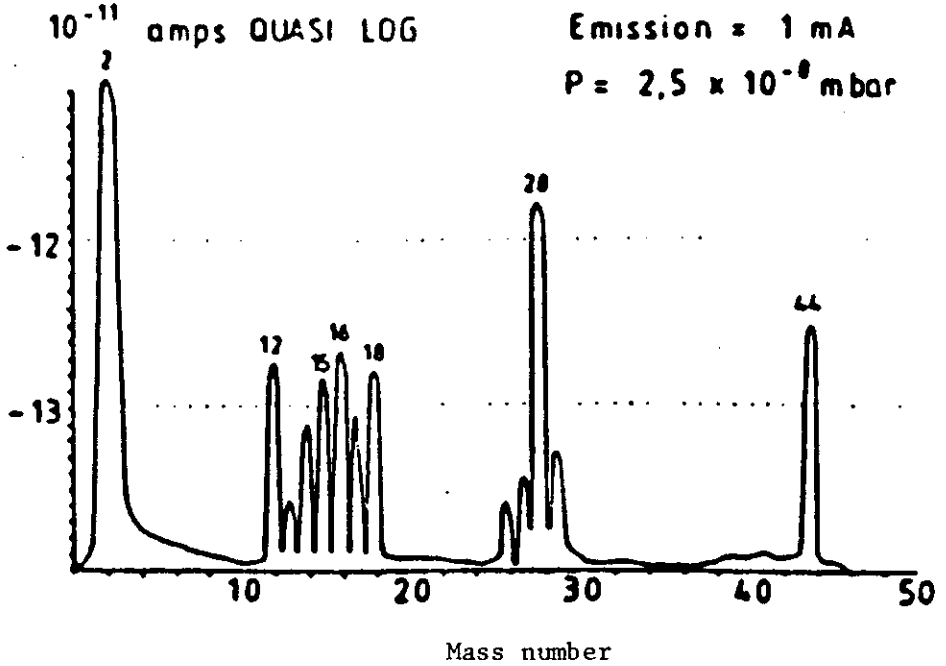

FIGURE 19b

The residual gas spectrum in the Argon Glow Discharged sector under the same conditions.

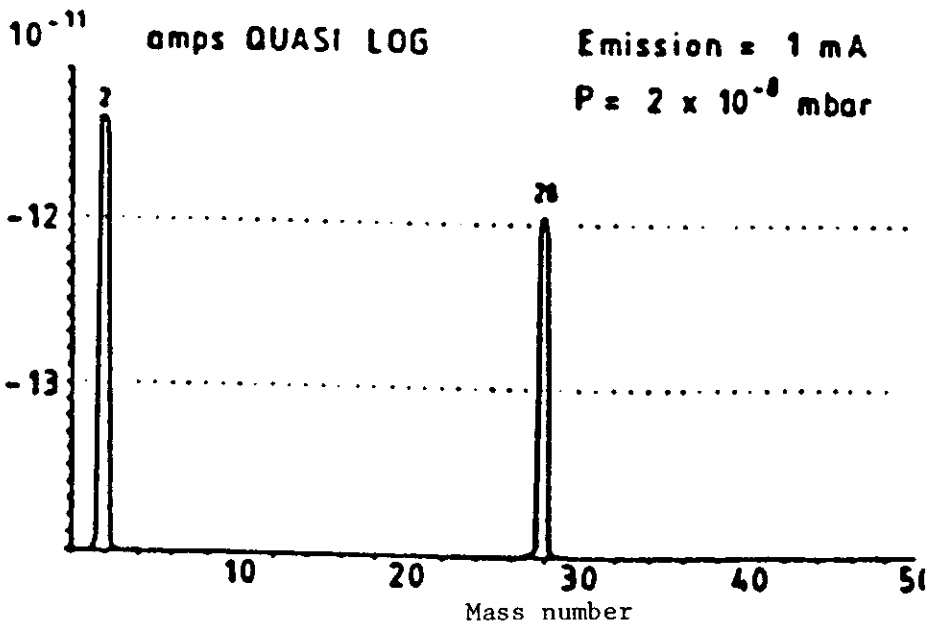

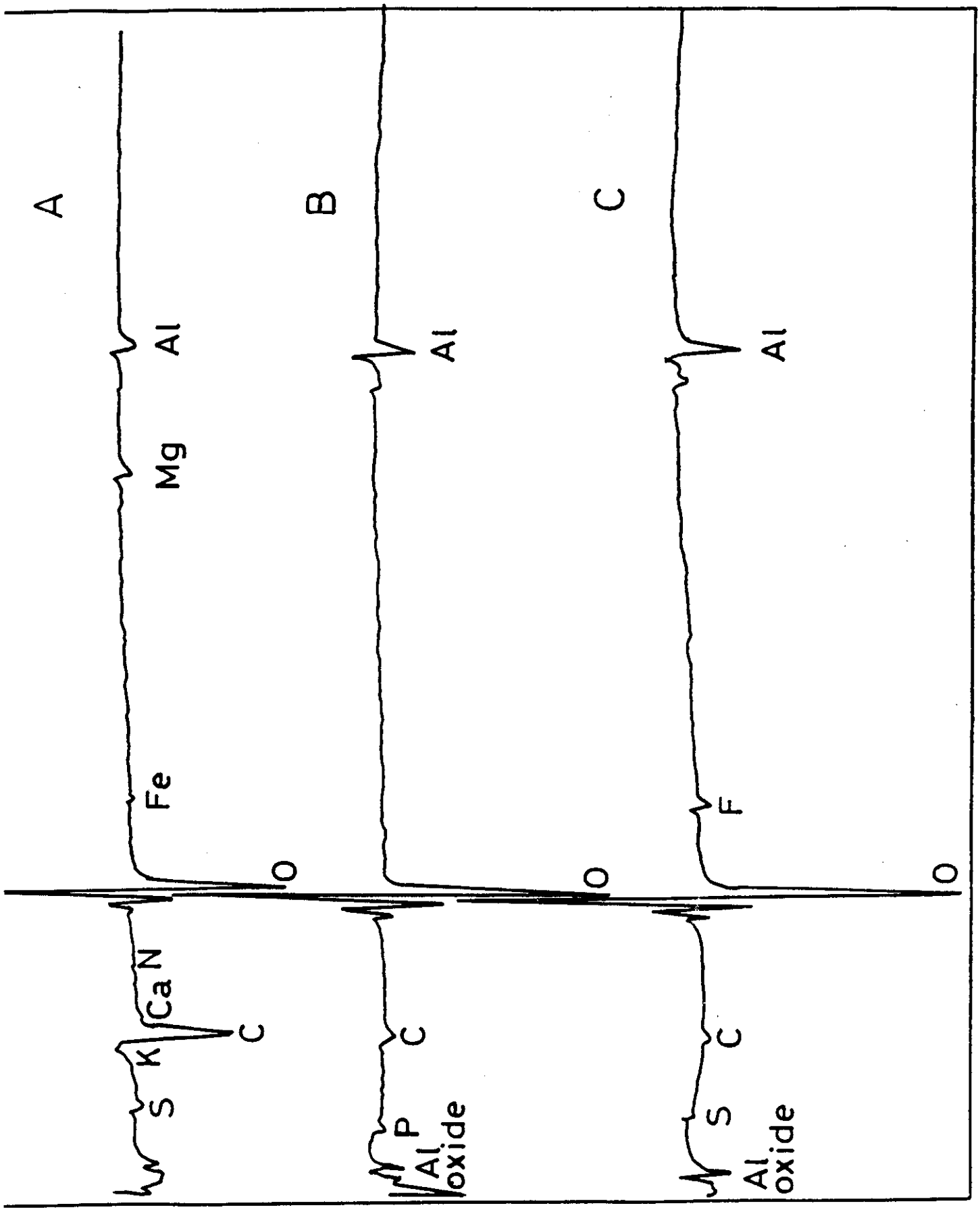

Figure 20

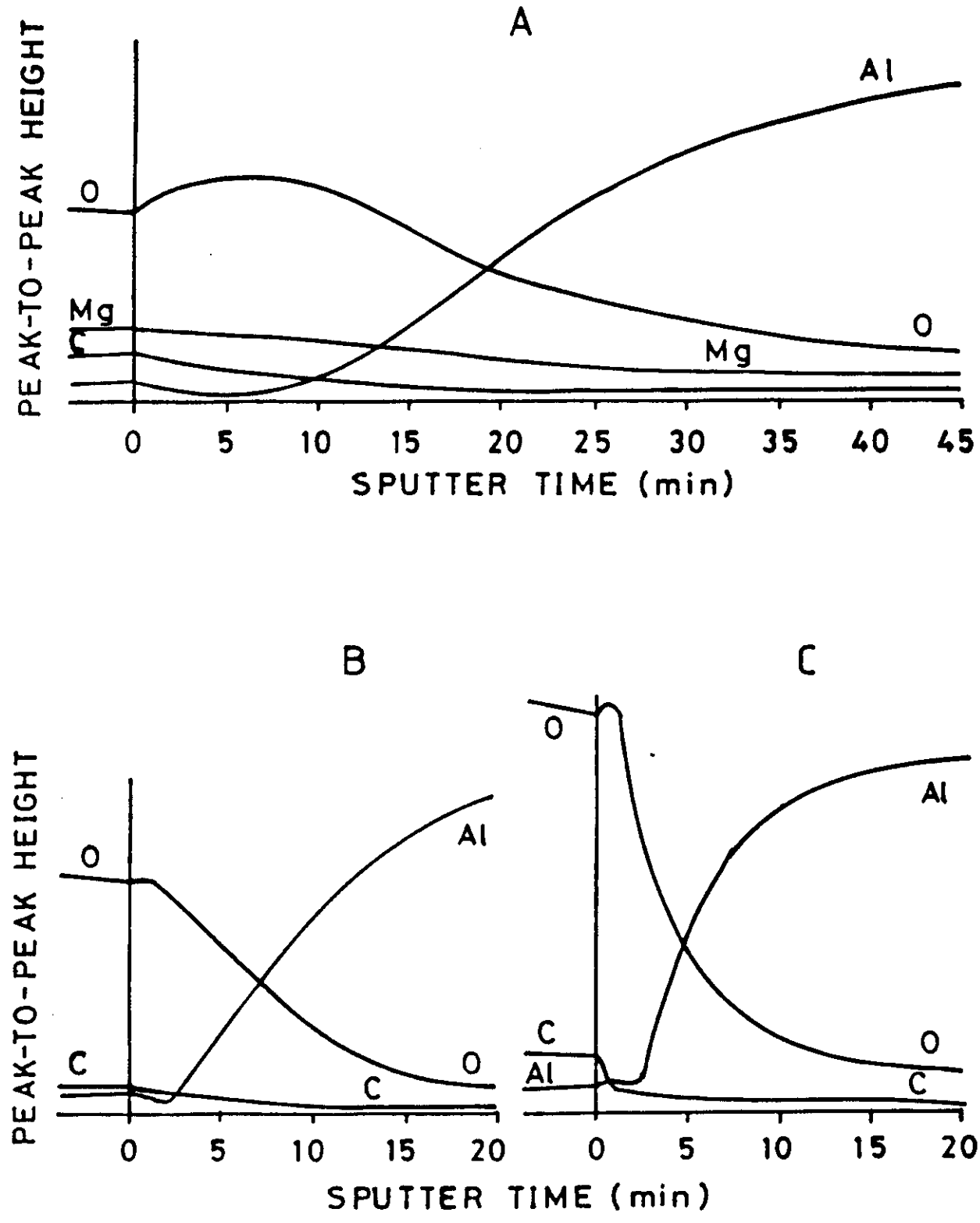
A
Al
O
Mg
O
Mg
PEAK-TO-PEAK HEIGHT
0 5 10 15 20 25 30 35 40 45
SPUTTER TIME (min)
B
C
O
Al
C
O
C
PEAK-TO-PEAK HEIGHT
0 5 10 15 20
O
Al
C
Al
O
C
0 5 10 15 20
SPUTTER TIME (min)

Figure 21

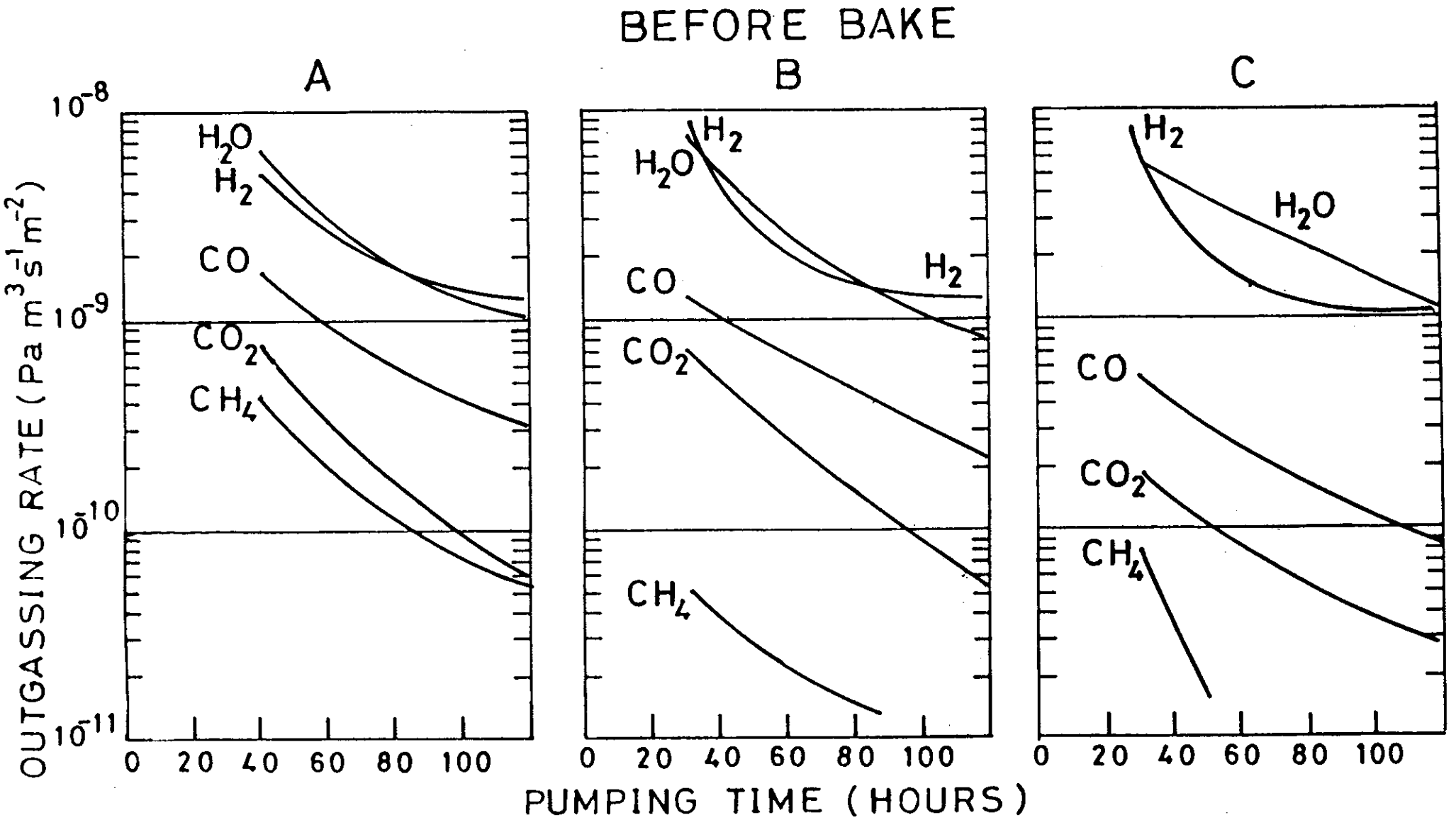
BEFORE BAKE
A
B
C
10^{-8}
10^{-9}
10^{-10}
10^{-11}
OUTGASSING RATE (Pa $m^3 s^{-1} m^{-2}$)
H_2O
H_2
CO
CO_2
CH_4
0 20 40 60 80 100
PUMPING TIME (HOURS)

Figure 22

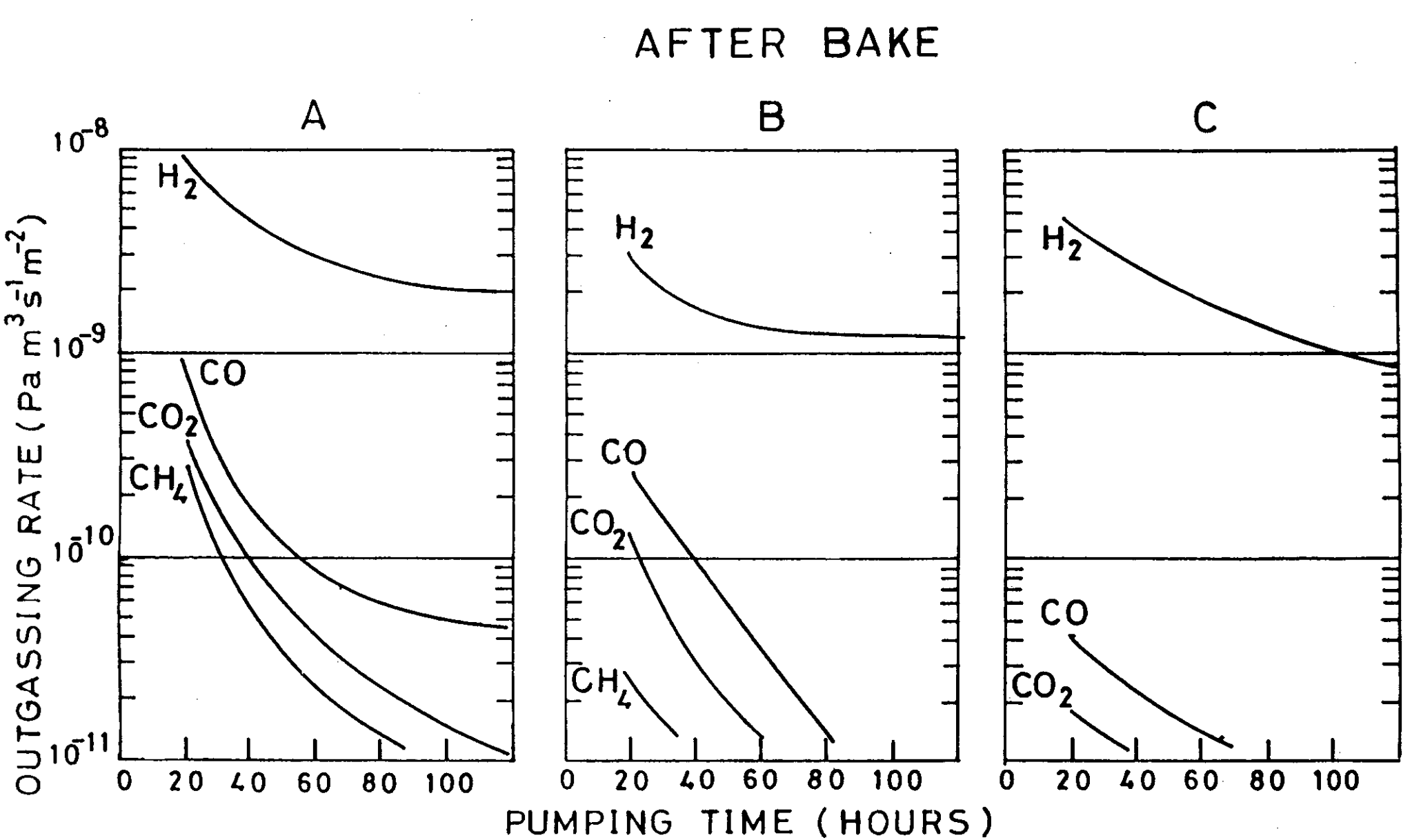
AFTER BAKE
A
B
C
10^{-8}
10^{-9}
10^{-10}
10^{-11}
H_2
CO
CO_2
CH_4
OUTGASSING RATE (Pa $m^3 s^{-1} m^{-2}$)
0 20 40 60 80 100
PUMPING TIME (HOURS)

Figure 23

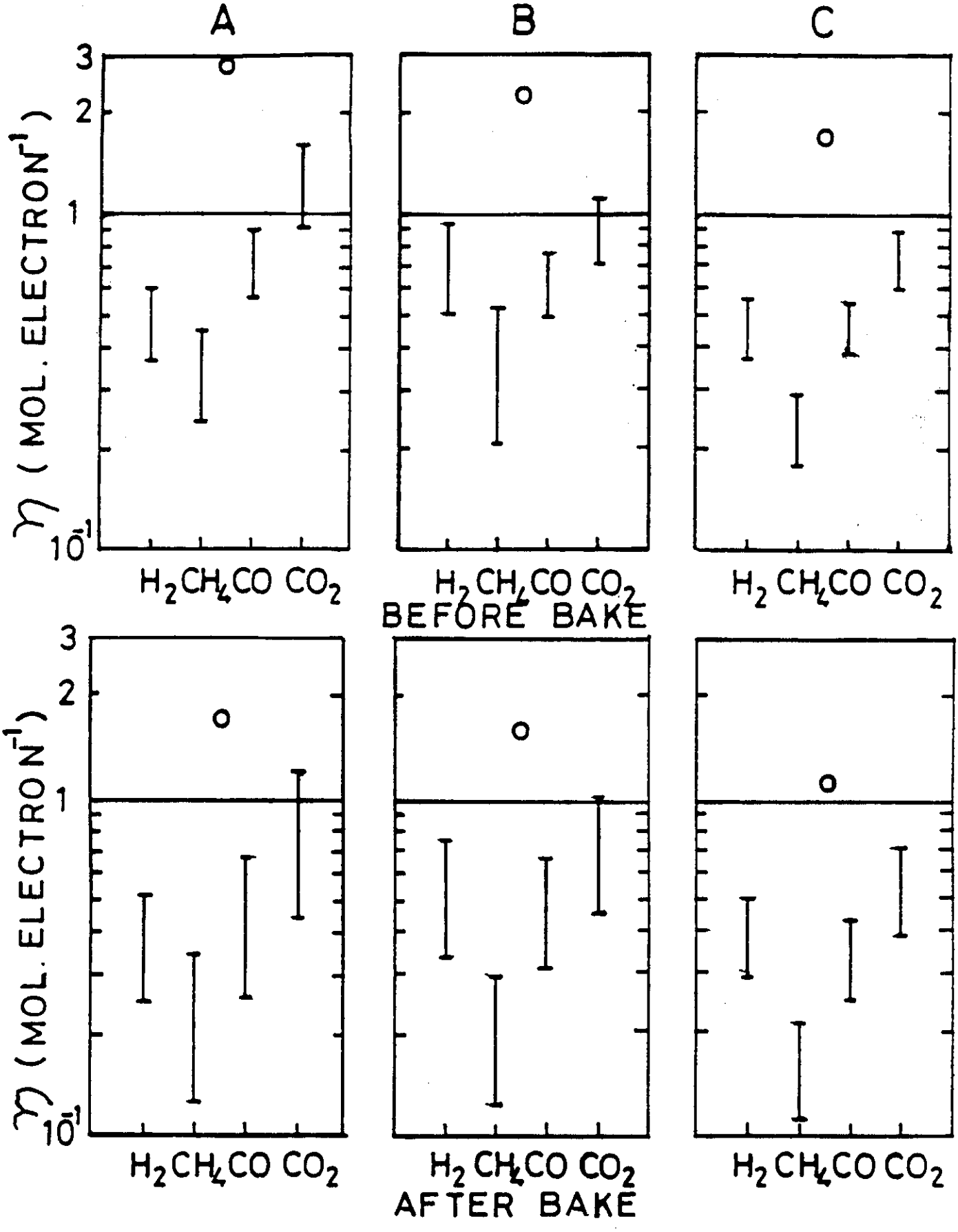
A
B
C
3
2
1
10^{-1}
η (MOL. ELECTRON^{-1})
H_2 CH_4 CO CO_2
BEFORE BAKE
AFTER BAKE

Figure 24

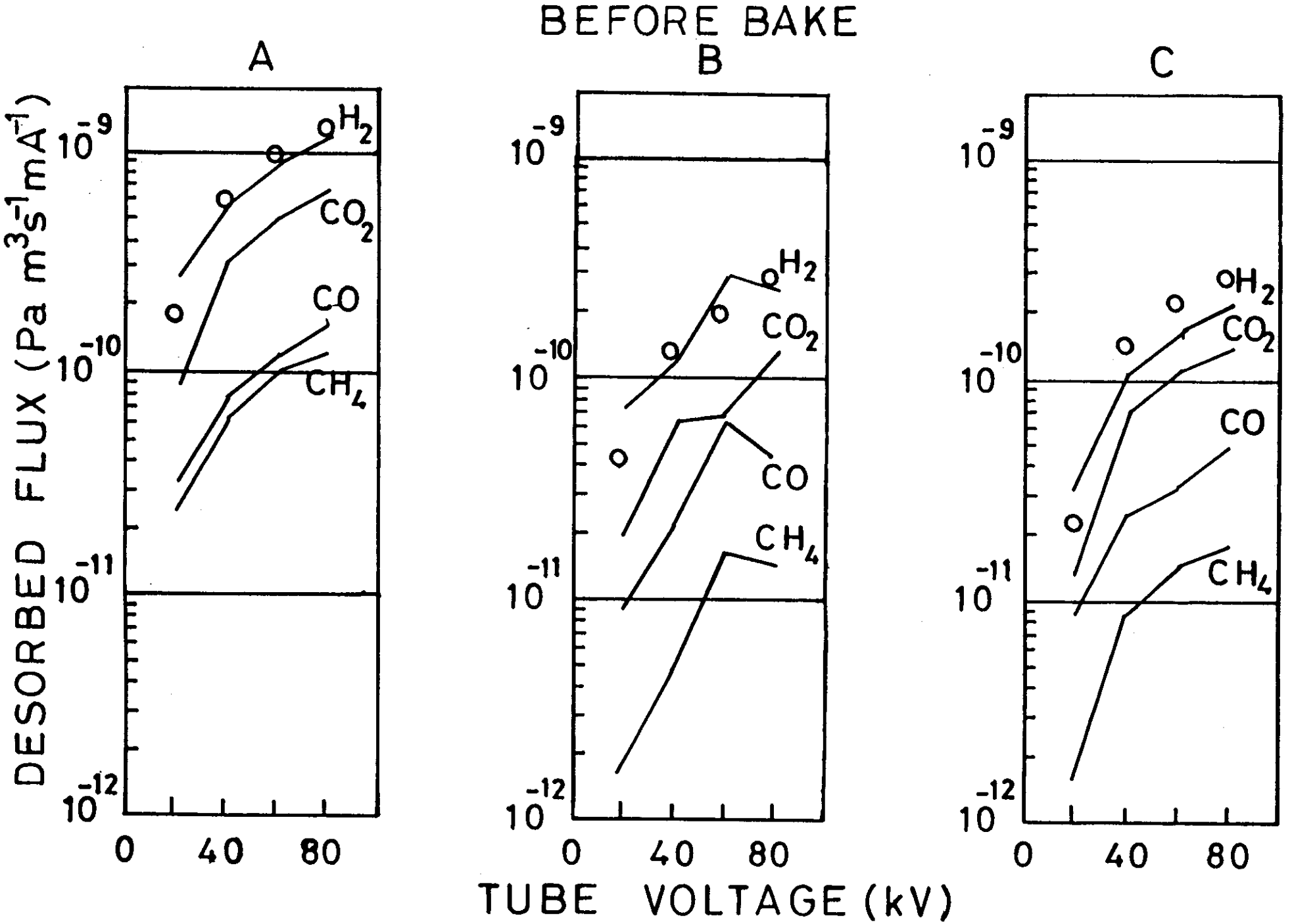
BEFORE BAKE
A
B
C
DESORBED FLUX (Pa m3s-1mA-1)
10-9
10-10
10-11
10-12
H2
CO2
CO
CH4
0
40
80
TUBE VOLTAGE (kV)

Figure 25

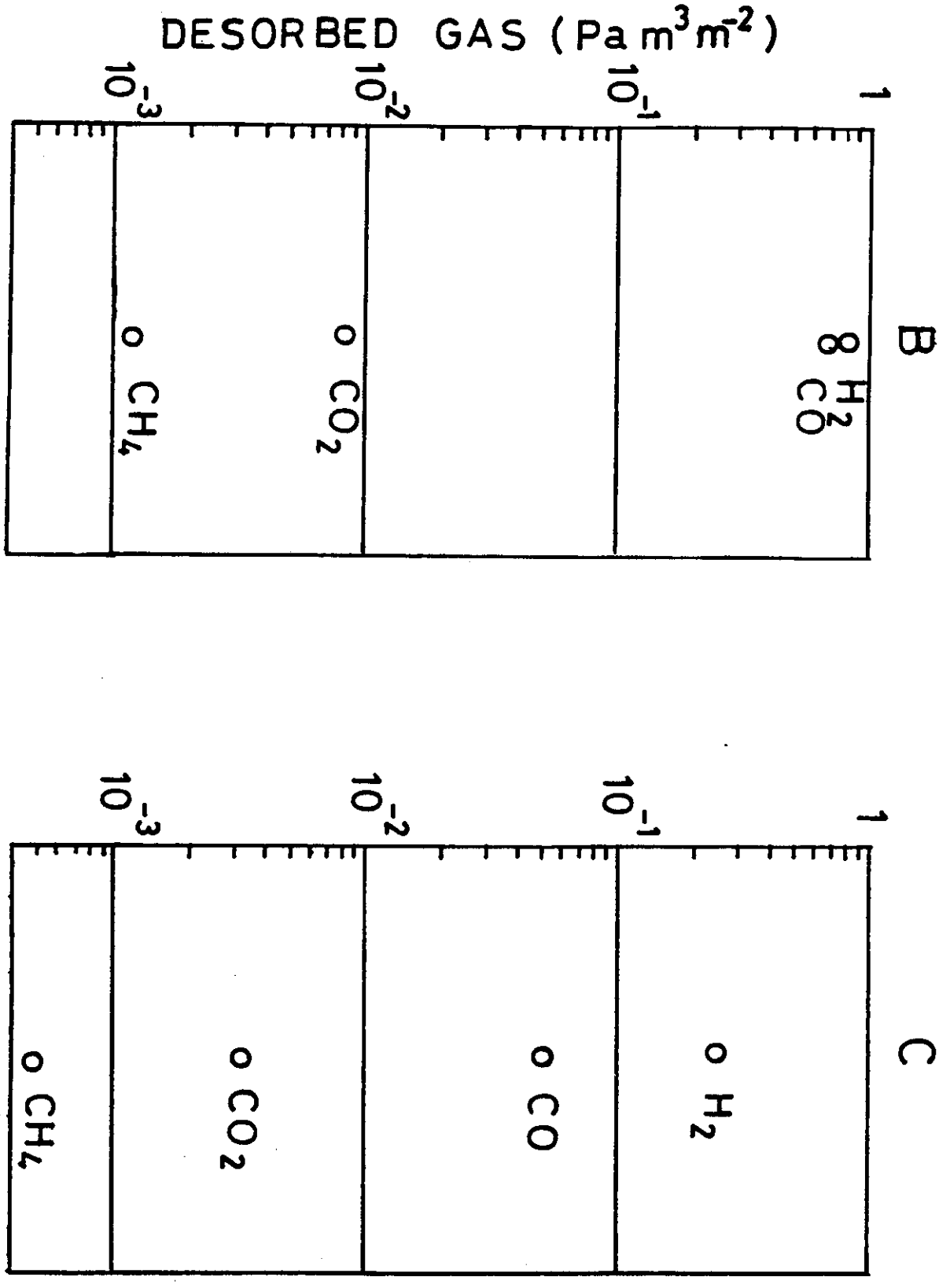
DESORBED GAS (Pa m³ m⁻²)
10⁻³
10⁻²
10⁻¹
1
B
o CH₄
o CO₂
o H₂
o CO
C
o CH₄
o CO₂
o CO
o H₂

Figure 27

TREATMENT A

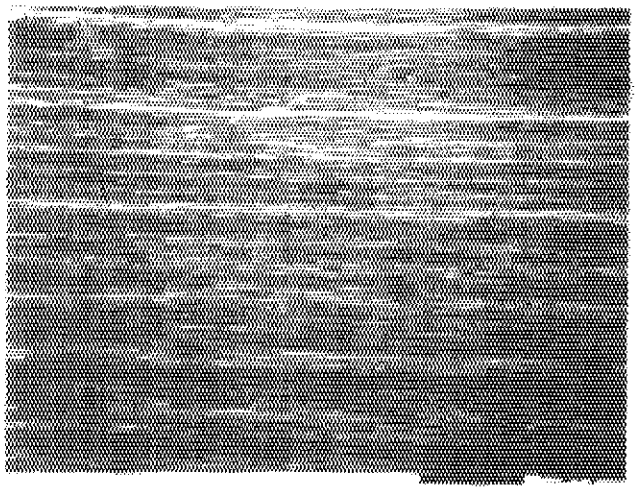

x 700

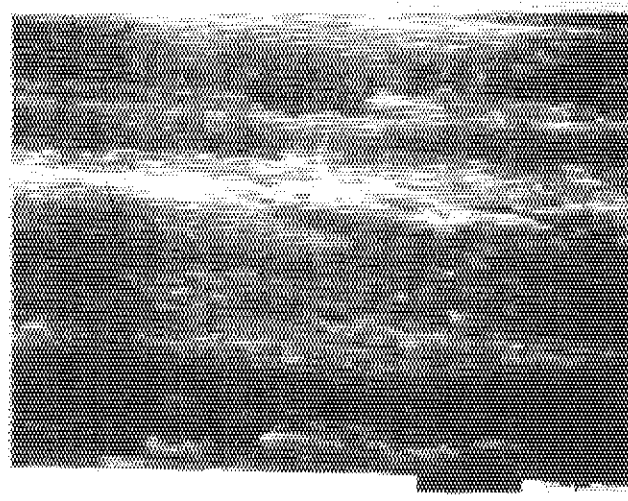

x 3500

TREATMENT B

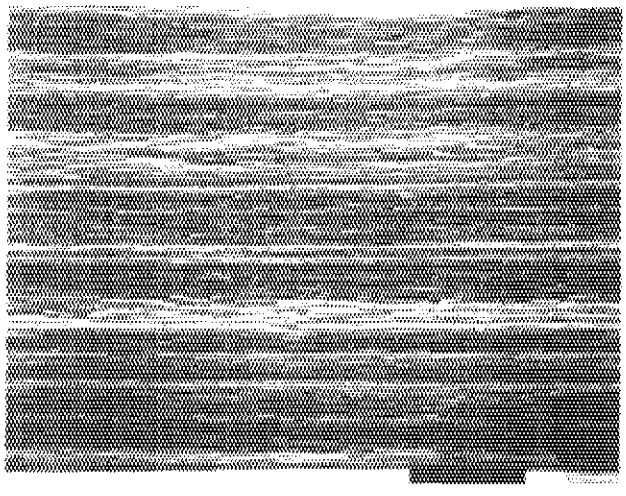

x 700

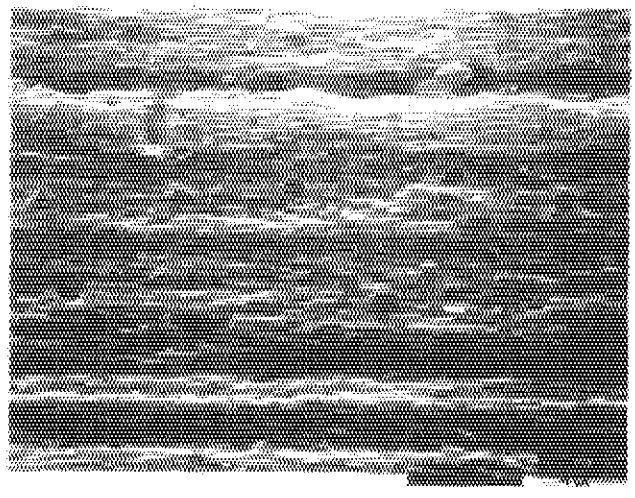

x 3500

TREATMENT C

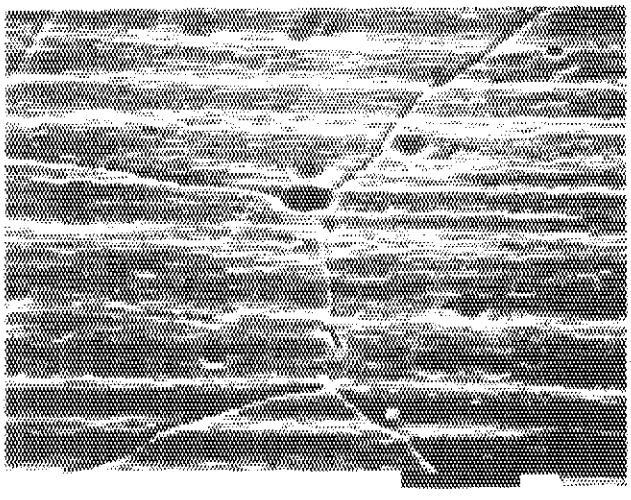

x 700

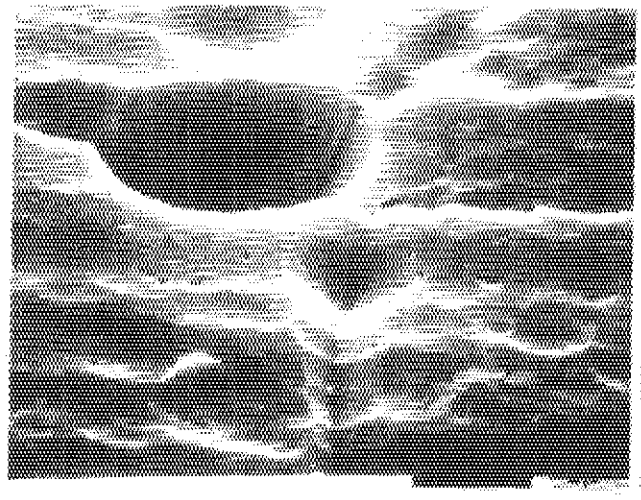

x 3500

FIGURE 28

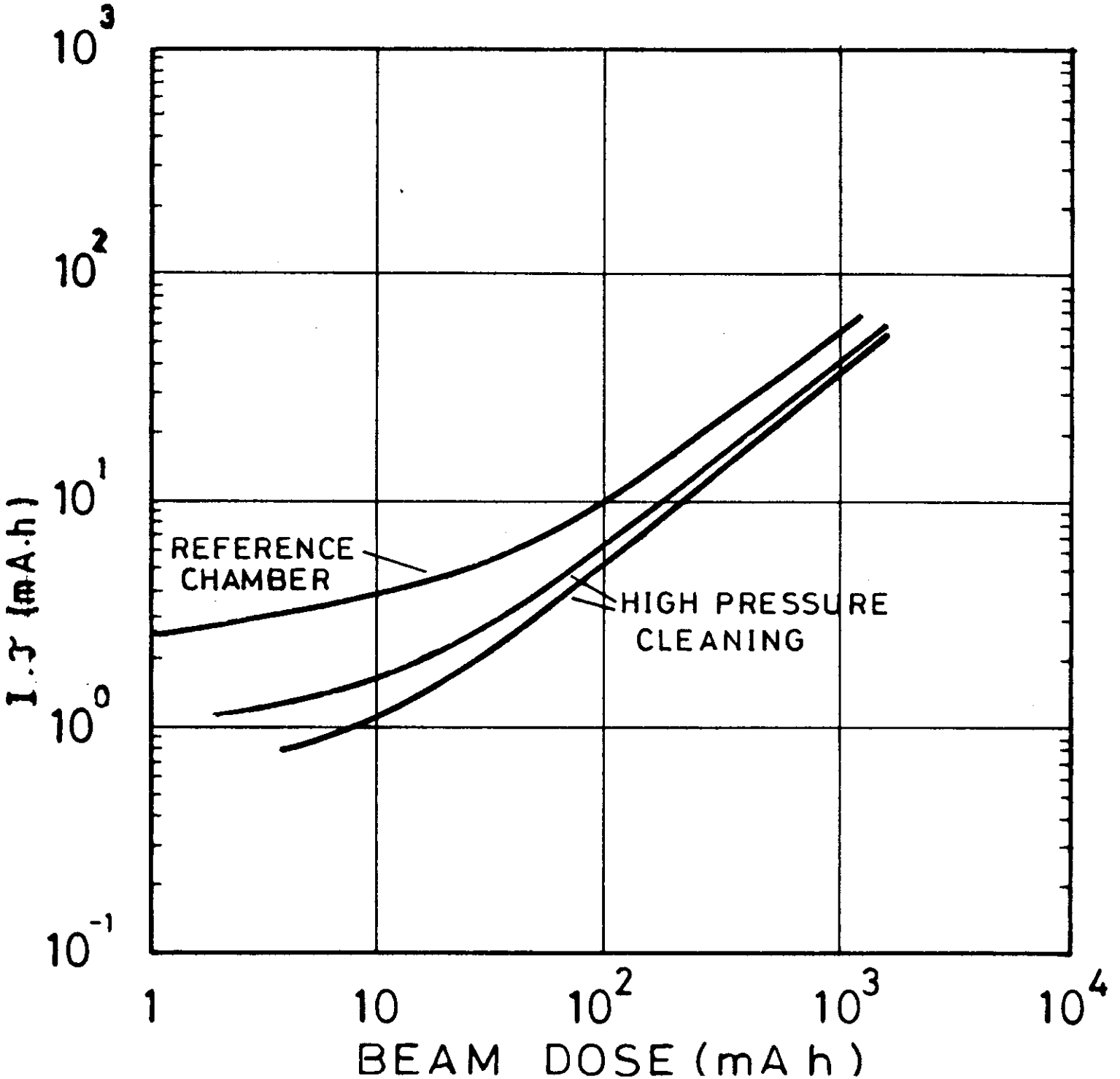
10^3
10^2
10^1
10^0
10^{-1}
I.τ (mA·h)
REFERENCE CHAMBER
HIGH PRESSURE CLEANING
1
10
10^2
10^3
10^4
BEAM DOSE (mA h)

Figure 29